Zhichao Fan
AML,
Department of Engineering Mechanics,
Tsinghua University,
Beijing 100084, China;
Center for Mechanics and Materials,
Tsinghua University,
Beijing 100084, China

Jian Wu[1]
AML,
Department of Engineering Mechanics,
Tsinghua University,
Beijing 100084, China;
Center for Mechanics and Materials,
Tsinghua University,
Beijing 100084, China
e-mail: wujian@tsinghua.edu.cn

Qiang Ma
AML,
Department of Engineering Mechanics,
Tsinghua University,
Beijing 100084, China;
Center for Mechanics and Materials,
Tsinghua University,
Beijing 100084, China

Yuan Liu
AML,
Department of Engineering Mechanics,
Tsinghua University,
Beijing 100084, China;
Center for Mechanics and Materials,
Tsinghua University,
Beijing 100084, China

Yewang Su
State Key Laboratory of Nonlinear Mechanics,
Institute of Mechanics,
Chinese Academy of Sciences,
Beijing 100190, China

Keh-Chih Hwang[1]
AML,
Department of Engineering Mechanics,
Tsinghua University,
Beijing 100084, China;
Center for Mechanics and Materials,
Tsinghua University,
Beijing 100084, China
e-mail: huangkz@tsinghua.edu.cn

Post-Buckling Analysis of Curved Beams

Stretchability of the stretchable and flexible electronics involves the post-buckling behaviors of internal connectors that are designed into various shapes of curved beams. The linear displacement–curvature relation is often used in the existing post-buckling analyses. Koiter pointed out that the post-buckling analysis needs to account for curvature up to the fourth power of displacements. A systematic method is established for the accurate post-buckling analysis of curved beams in this paper. It is shown that the nonlinear terms in curvature should be retained, which is consistent with Koiter's post-buckling theory. The stretchability and strain of the curved beams under different loads can be accurately obtained with this method. [DOI: 10.1115/1.4035534]

Keywords: post-buckling, stretchability, curved beam, curvature, finite deformation

1 Introduction

Curved beams have simple geometry and facilitative fabrication and are widely used in the fields of electronic, aerospace, and architecture. Recently, curved beams are treated as internal connectors of stretchable electronics due to their high stretchability with small strain [1–13]. There are many functional stretchable and flexible electronics based on different shapes of curved beams, such as epidermal health/wellness monitors [14–18], sensitive electronic skins [19–23], and spherical-shaped digital cameras [24–26]. The post-buckling behaviors, especially lateral and out-of-plane buckling, provide the flexibility and stretchability of the electronics [27], which are the essential properties of a robust technology of assembling various microstructures [28–30].

There are many researchers studying up on the stability of planar curved beams. Timoshenko and Gere [31] presented initial buckling behaviors of circular beams. The analytical models for post-buckling behaviors of the inextensible ring under uniform radial pressure were developed by Carrier [32] and Budiansky [33]. A systematic variational approach of space curved beams was developed by Liu and Lu and employed on buckling behavior and critical load of the serpentine structure [34]. Many results of the post-buckling behaviors of curved beams are obtained by the semi-analytical energy approach and finite-element method

(FEM) [35,36]. Koiter's approach of energy minimization for post-buckling expanded the potential energy to the fourth power of displacement because the third and fourth power terms actually govern post-buckling [37–39], which require the elongation and curvature that at least express the third power of displacement.

This paper presents a systematic study on post-buckling of curved beam, the nonlinear relations between the deformation components (elongation and curvatures) and displacements are derived, and the perturbation method is used to obtain the analytical solution of the post-buckling behaviors of curved beams.

2 Deformation of Curved Beam

2.1 The Initial and Deformed Curved Beams. The material points on the centroid line of the initial curved beam are denoted by $\tilde{P}(S)$ (Fig. 1), where S is the arc-length of centroid line. The local triad vectors at the centroid line of the curved beam are orthogonal unit vectors $E_i(i = 1, 2, 3)$. E_1 and E_2 are along two lines of symmetry of the cross section of beam (Fig. 1). E_3 is the unit vector along the tangential direction of the centroid line and can be given as

$$E_3 = \frac{\mathrm{d}\tilde{P}}{\mathrm{d}S} \tag{2.1}$$

The curvature of the curved beam was defined by Love [40] as

$$\frac{\mathrm{d}E_i}{\mathrm{d}S} = K \times E_i \quad (i = 1, 2, 3) \tag{2.2}$$

where the curvature $K = K_1E_1 + K_2E_2 + K_3E_3$, K_1 and K_2 are the curvatures along the axes in cross section, and K_3 denotes the twist along the tangential direction of the centroid line.

The centroid line of curved beam is deformed from $\tilde{P}$ to $\tilde{p} = \tilde{P} + U$, where U is the displacement of the beam. The local triad vectors of the deformed curved beam are $e_i(i = 1, 2, 3)$, where e_1 and e_2 are the orthogonal unit vectors in the cross section of deformed curved beam, and e_3 is the unit vector along the tangential direction of the centroid line of deformed beam, which is defined as

$$e_3 = \frac{\mathrm{d}\tilde{p}}{\mathrm{d}s} \tag{2.3}$$

where s is the arc-length coordinate of the deformed beam, which is the function of the arc-length of initial curved beam, S. The elongation of the deformed beam, λ, can be obtained from

$$\lambda = \frac{\mathrm{d}s}{\mathrm{d}S} \tag{2.4}$$

The curvature of the deformed curved beam also can be given as [40]

$$\frac{\mathrm{d}e_i}{\mathrm{d}s} = \kappa \times e_i \quad (i = 1, 2, 3) \tag{2.5}$$

where $\kappa = \kappa_1e_1 + \kappa_2e_2 + \kappa_3e_3$, κ_1 and κ_2 are the components of curvature along sectional vectors e_1 and e_2, respectively, and κ_3 denotes the twist along the tangent direction, e_3. Here, the twist angle, ϕ, is defined with κ_3 as

$$\phi = \int \kappa_3 \mathrm{d}s \tag{2.6}$$

where the axis of the twist angle changes with the location.

2.2 Equilibrium Equations and Constitutive Relation of Curved Beam. The internal force, $t = t_ie_i$, and moment, $m = m_ie_i$, of the curved beam satisfy the following equilibrium equations [41]:

$$\frac{\mathrm{d}t}{\mathrm{d}s} + p = 0$$
$$\frac{\mathrm{d}m}{\mathrm{d}s} + e_3 \times t + q = 0 \tag{2.7}$$

where $p = p_ie_i$ and $q = q_ie_i$ are the distributed force and moment per unit length in the deformed beam, respectively. The derivative symbols have the relation, $(1/\lambda)(\mathrm{d}()/\mathrm{d}S) = (\mathrm{d}()/\mathrm{d}s)$.

The internal force, t_3, is conjugate with the elongation, λ, and has the constitutive relation

$$t_3 = EA(\lambda - 1) \tag{2.8}$$

where E and A are the elastic modulus and the cross section area of the beam, respectively.

The moment, m, is not conjugate with the curvature, κ, but it is conjugate with the Lagrangian curvature, $\hat{\kappa}$, which is defined as

$$\frac{\mathrm{d}e_i}{\mathrm{d}S} = \hat{\kappa} \times e_i \quad (i = 1, 2, 3) \tag{2.9}$$

where the Lagrangian curvature, $\hat{\kappa}$, has the relation with curvature, κ, as $\hat{\kappa} = \lambda\kappa$.

The constitutive relation between Lagrangian curvatures (abbreviated hereafter simply to curvatures) and moments is

$$m_1 = EI_1(\hat{\kappa}_1 - K_1)$$
$$m_2 = EI_2(\hat{\kappa}_2 - K_2) \tag{2.10}$$
$$m_3 = GJ(\hat{\kappa}_3 - K_3)$$

where G is the shear modulus of the beam, I_1 and I_2 are the section area moment of inertia about the local coordinates, and J is the polar moment of inertia of the cross section of beam.

The components of the equilibrium equation expressed with the components of internal forces, moments, and the curvatures can be given as

$$\frac{\mathrm{d}t_i}{\mathrm{d}S} + \epsilon_{ijk}\hat{\kappa}_jt_k + \lambda p_i = 0 \quad (i = 1, 2, 3)$$
$$\frac{\mathrm{d}m_i}{\mathrm{d}S} + \epsilon_{ijk}\hat{\kappa}_jm_k - \epsilon_{ij3}\lambda t_j + \lambda q_i = 0 \quad (i = 1, 2, 3) \tag{2.11}$$
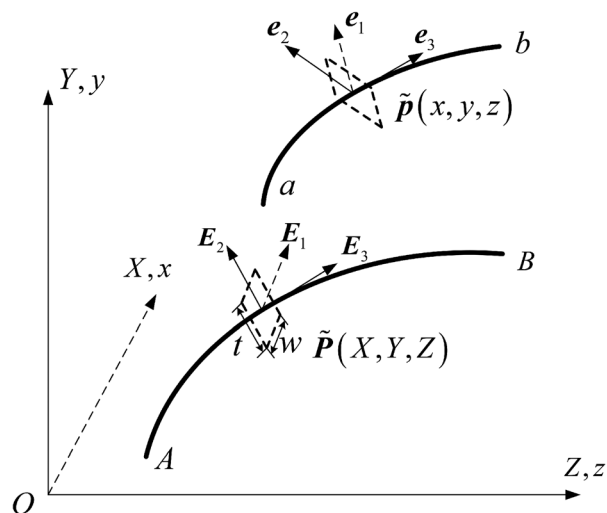

Fig. 1 Schematic illustration of initial and deformed curved beam

where ϵ_{ijk} are the components of Eddington tensor.

3 The Deformation Variables in Terms of Displacement for Planar Curved Beam

The planar curved beam, which has only one nonzero component of initial curvature, K_1, is widely used. We will focus on the planar curved beam in Secs. 3–7. The displacement, U, can decompose in the local coordinates, $E_i (i = 1, 2, 3)$, as $U = U_1 E_1 + U_2 E_2 + U_3 E_3$. The elongation defined by Eq. (2.4) can be expressed through the components of the displacement as

$$\lambda = \left\{ 1 + 2\left(\frac{dU_3}{dS} + U_2 K_1\right) + \left[\left(\frac{dU_1}{dS}\right)^2 + \left(\frac{dU_2}{dS} - U_3 K_1\right)^2 + \left(\frac{dU_3}{dS} + U_2 K_1\right)^2\right] \right\}^{\frac{1}{2}}$$
(3.1)

The relations between the local triads on the initial and deformed curved beams are given by the coefficients a_{ij} as

$$e_i = a_{ij} E_j \quad (i = 1, 2, 3)$$
(3.2)

E_3 and e_3 are along the tangent directions of the initial and deformed curved beams, respectively. By substituting Eqs. (2.1) and (2.3) into Eq. (3.2), the coefficients, $a_{3j}(j = 1, 2, 3)$, can be derived as

$$a_{31} = \frac{1}{\lambda}\frac{dU_1}{dS}, \quad a_{32} = \frac{1}{\lambda}\left(\frac{dU_2}{dS} - U_3 K_1\right),$$
$$a_{33} = \frac{1}{\lambda}\left(1 + \frac{dU_3}{dS} + U_2 K_1\right)$$
(3.3)

The local coordinates, $e_i (i = 1, 2, 3)$ and $E_i (i = 1, 2, 3)$, are orthonormal (i.e., $e_i \cdot e_j = \delta_{ij}$ and $E_i \cdot E_j = \delta_{ij}$), which lead the coefficients, a_{ij}, to satisfy the following equations:

$$a_{i1}^2 + a_{i2}^2 + a_{i3}^2 = 1 \quad (i = 1, 2, 3)$$
$$a_{ik} a_{jk} = 0 \quad (i \neq j)$$
(3.4)

The relations between the coefficients, $a_{ij}(i = 1, 2, j = 1, 2, 3)$, the displacements, U_i, and the twist angle, ϕ, are complicated and cannot be explicitly expressed as Eq. (3.3). Substitution of Eqs. (3.1) and (3.3) into Eq. (3.4) and expansion of the coefficients, a_{ij}, to the powers of generalized displacements lead to

$$\{a_{ij}\} = \begin{Bmatrix} 1 & 0 & 0 \\ 0 & 1 & 0 \\ 0 & 0 & 1 \end{Bmatrix}$$
$$+ \begin{Bmatrix} 0 & \psi^{[1]} & -\dfrac{dU_1}{dS} \\ -\psi^{[1]} & 0 & -\dfrac{dU_2}{dS} + U_3 K_1 \\ \dfrac{dU_1}{dS} & \dfrac{dU_2}{dS} - U_3 K_1 & 0 \end{Bmatrix}$$
$$+ \left\{a_{ij}^{\langle 2 \rangle}\right\} + \left\{a_{ij}^{\langle 3 \rangle}\right\} + \{\cdots\} \quad (i, j = 1, 2, 3)$$
(3.5)

where $\psi^{[1]} = \phi - \int K_1 (dU_1/dS) dS$, and the superscripts $\langle 2 \rangle$ and $\langle 3 \rangle$ in $a_{ij}^{\langle 2 \rangle}$ and $a_{ij}^{\langle 3 \rangle}$ refer to the second and third power of generalized displacements (i.e., U_i and ϕ). They are given in Appendix A, and $\{\cdots\}$ are the terms of the fourth and higher power of displacements and twist angle.

After substituting Eqs. (3.2) and (3.5) into Eq. (2.9), the curvatures can be expressed in terms of generalized displacements as

$$\begin{Bmatrix} \hat{\kappa}_1 \\ \hat{\kappa}_2 \\ \hat{\kappa}_3 \end{Bmatrix} = \begin{Bmatrix} K_1 \\ 0 \\ 0 \end{Bmatrix} + \begin{Bmatrix} -\dfrac{d^2 U_2}{dS^2} + \dfrac{d(U_3 K_1)}{dS} \\ \dfrac{d^2 U_1}{dS^2} - \psi^{[1]} K_1 \\ \dfrac{d\phi}{dS} \end{Bmatrix} + \left\{\hat{\kappa}_i^{\langle 2 \rangle}\right\}$$
$$+ \left\{\hat{\kappa}_i^{\langle 3 \rangle}\right\} + \{\cdots\}$$
(3.6)

where $\hat{\kappa}_i^{\langle 2 \rangle}$ and $\hat{\kappa}_i^{\langle 3 \rangle}$ are the second and third power of displacements, U_i, and twist angle, ϕ, which are given in Appendix A. The nonlinear terms (i.e., $\hat{\kappa}_i^{\langle 2 \rangle}$ and $\hat{\kappa}_i^{\langle 3 \rangle}$) are important for the analysis of the post-buckling behaviors of the curved beams based on the Koiter's theory. As far as the authors are aware, the power expansion of deformation for Euler–Bernoulli curved beams (without assuming inextensibility of the beams) is a new result. The results obtained by Su et al. [41] for straight beams follow as a special case.

4 The Perturbation Solution for Post-Buckling of the Planar Curved Beam

The planar curved beam will be buckling in-plane or out-of-plane due to the planar loads (e.g., $p_1 = 0$). The method of perturbation is used to solve differential equations (2.11) substituted with variables of the deformation and displacement, where a small ratio, a, of the maximum deflection to the characteristic length (e.g., the beam length, L_S, or the initial curvature radius of beam, R) is introduced. The generalized displacements from buckling, expanded to the powers of a, can be written as

$$U_1 = a U_{1(1)} + a^2 U_{1(2)} + a^3 U_{1(3)} + O(a^4) L_S$$
$$U_2 = a U_{2(1)} + a^2 U_{2(2)} + a^3 U_{2(3)} + O(a^4) L_S$$
$$U_3 = a U_{3(1)} + a^2 U_{3(2)} + a^3 U_{3(3)} + O(a^4) L_S$$
$$\phi = a \phi_{(1)} + a^2 \phi_{(2)} + a^3 \phi_{(3)} + O(a^4)$$
(4.1)

By substituting Eq. (4.1) into Eqs. (3.1) and (3.6), the elongation and curvatures can be also expanded to the powers of the small ratio, a, as

$$\lambda = 1 + a\lambda_{(1)} + a^2 \lambda_{(2)} + a^3 \lambda_{(3)} + O(a^4)$$
(4.2)

$$\hat{\kappa}_i = \hat{\kappa}_{i(0)} + a\hat{\kappa}_{i(1)} + a^2 \hat{\kappa}_{i(2)} + a^3 \hat{\kappa}_{i(3)} + O(a^4) L_S^{-1} \quad (i = 1, 2, 3)$$
(4.3)

where $\hat{\kappa}_{1(0)} = K_1$, $\hat{\kappa}_{2(0)} = \hat{\kappa}_{3(0)} = 0$, $\lambda_{(k)}$ and $\hat{\kappa}_{i(k)}$ are the functions of generalized displacements, and

$$\lambda_{(1)} = \frac{dU_{3(1)}}{dS} + U_{2(1)} K_1$$
(4.4)

$$\hat{\kappa}_{1(1)} = -\frac{d^2 U_{2(1)}}{dS^2} + \frac{d(U_{3(1)} K_1)}{dS}$$
$$\hat{\kappa}_{2(1)} = \frac{d^2 U_{1(1)}}{dS^2} - \psi^{[1]}_{(1)} K_1$$
$$\hat{\kappa}_{3(1)} = \frac{d\phi_{(1)}}{dS}$$
(4.5)

where $\psi^{[1]}_{(1)} = \phi_{(1)} - \int K_1 (dU_{1(1)}/dS) dS$.

The coefficient, a_{ij}, can be expanded to the powers of the small ratio, a, as

$$a_{ij} = 1 + a^2 a_{ij(2)} + a^3 a_{ij(3)} + O(a^4) \quad (i = j)$$
$$a_{ij} = a a_{ij(1)} + a^2 a_{ij(2)} + a^3 a_{ij(3)} + O(a^4) \quad (i \neq j)$$
(4.6)

where $a_{ij(k)}$ are the functions of generalized displacements

$$a_{ij(1)} = \left\{ \begin{array}{ccc} 0 & \psi^{[1]}_{(1)} & -\dfrac{dU_{1(1)}}{dS} \\[2mm] -\psi^{[1]}_{(1)} & 0 & -\dfrac{dU_{2(1)}}{dS} + U_{3(1)}K_1 \\[2mm] \dfrac{dU_{1(1)}}{dS} & \dfrac{dU_{2(1)}}{dS} - U_{3(1)}K_1 & 0 \end{array} \right\}$$
(4.7)

The expressions of $\lambda_{(k)}$, $\hat{\kappa}_{i(k)}$, and $a_{ij(k)}$ for $k = 2$ are given in Appendix B.

Substituting Eqs. (4.2) and (4.3) into constitutive relations (2.8) and (2.10) and considering the equilibrium equations, the internal forces and moments can be expanded to powers of the small ratio a as

$$t_i = t_{i(0)} + a t_{i(1)} + a^2 t_{i(2)} + a^3 t_{i(3)} + O(a^4)EA \quad (4.8)$$

$$m_i = m_{i(0)} + a m_{i(1)} + a^2 m_{i(2)} + a^3 m_{i(3)} + O(a^4)EI_1 L_S^{-1} \quad (4.9)$$

where $t_{i(0)}$ and $m_{i(0)}$ are the forces and moments at the onset of buckling, and the relation between $t_{3(k)}$, $m_{i(k)}$, and $\lambda_{(k)}$, $\hat{\kappa}_{i(k)}$ ($k \geq 1$) can be written as

$$\begin{aligned} t_{3(k)} &= EA\lambda_{(k)} \\ m_{1(k)} &= EI_1 \hat{\kappa}_{1(k)} \\ m_{2(k)} &= EI_2 \hat{\kappa}_{2(k)} \\ m_{3(k)} &= GJ \hat{\kappa}_{3(k)} \end{aligned}$$
(4.10)

After substituting the forces (4.8) and moments (4.9), equilibrium equations (2.11) can be decomposed as

$$\frac{dt_{i(0)}}{dS} + \epsilon_{ijk}\hat{\kappa}_{j(0)}t_{k(0)} + p_{i(0)} = 0 \quad (i = 1, 2, 3)$$
$$\frac{dm_{i(0)}}{dS} + \epsilon_{ijk}\hat{\kappa}_{j(0)}m_{k(0)} - \epsilon_{ij3}t_{j(0)} + q_{i(0)} = 0 \quad (i = 1, 2, 3)$$
(4.11)

and

$$\frac{dt_{i(n)}}{dS} + \sum_{l=0}^{l=n}\left(\epsilon_{ijk}\hat{\kappa}_{j(l)}t_{k(n-l)} + \lambda_{(l)}p_{i(n-l)}\right) = 0$$
$$(i = 1, 2, 3; n = 1, 2, 3, \ldots)$$
$$\frac{dm_{i(n)}}{dS} + \sum_{l=0}^{l=n}\left(\epsilon_{ijk}\hat{\kappa}_{j(l)}m_{k(n-l)} - \epsilon_{ij3}\lambda_{(l)}t_{j(n-l)} + \lambda_{(l)}q_{i(n-l)}\right) = 0$$
$$(i = 1, 2, 3; n = 1, 2, 3, \ldots)$$
(4.12)

where $\lambda_{(0)} = 1$, and the loads are expanded to the power series of a as

$$p_i = p_{i(0)} + a p_{i(1)} + a^2 p_{i(2)} + a^3 p_{i(3)} + O(a^4)EAL_S^{-1}$$
$$q_i = q_{i(0)} + a q_{i(1)} + a^2 q_{i(2)} + a^3 q_{i(3)} + O(a^4)EI_1 L_S^{-2}$$
(4.13)

where $p_{i(0)}$ and $q_{i(0)}$ are the critical loads at bifurcation point.

The differential equations in this section, in which internal forces and moments are substituted with deformation variables and displacements, are solved in the following steps.

Step 1: Solve Eq. (4.12) for $n = 1$ with the corresponding boundary conditions to determine the buckling mode for the leading order, $\lambda_{(1)}$, $\hat{\kappa}_{i(1)}$, and $U_{i(1)}$, of elongation, curvatures, and displacements, and the critical loads at the onset of buckling, $p_{i(0)}$ and $q_{i(0)}$.

Step 2: Solve Eq. (4.12) for $n = 2$ with the corresponding boundary conditions to determine the second order $\lambda_{(2)}$, $\hat{\kappa}_{i(2)}$, and $U_{i(2)}$ of elongation, curvatures, and displacements, and the increment of loads, $p_{i(1)}$ and $q_{i(1)}$.

Step 3: Solve Eq. (4.12) for $n = 3$ with the corresponding boundary conditions to determine the buckling mode for the third order $\lambda_{(3)}$ and $\hat{\kappa}_{i(3)}$ of elongation and curvatures, and the increment of loads, $p_{i(2)}$ and $q_{i(2)}$.

5 In-Plane Post-Buckling Behavior of Elastic Ring

As illustrated in Fig. 2, the uniform distributed radial load, p_2, which remains normal to the centroid line during the deformation, is applied on an elastic thin ring. The arc-length, S, is clockwise counted from A. The ring at A is simply supported, and the displacement along tangent direction at B is constrained, these boundary conditions can be written as

$$U_{i(n)}|_{S=0} = 0 \ (i = 1, 2, 3; n = 1, 2, 3, \ldots) \quad (5.1)$$

$$U_{3(n)}|_{S=\pi R} = 0 \ (n = 1, 2, 3, \ldots) \quad (5.2)$$

where $R = 1/K_1$ is the initial curvature radius of ring. The displacements, deformations, and forces/moments are periodical due to the periodical deformation of the ring, i.e.,

$$()|_{S=S_0} = ()|_{S=S_0+2\pi R}, \ (0 \leq S_0 \leq 2\pi R) \quad (5.3)$$

where () denotes λ, $\lambda_{(n)}$, $\hat{\kappa}_i$, $\hat{\kappa}_{i(n)}$, t_i, $t_{i(n)}$, m_i, $m_{i(n)}$, U_i, $U_{i(n)}$, ϕ, $\phi_{(n)}$, and a_{ij}, $a_{ij(n)}$.

The width of the ring section, w, is much larger than its thickness, t, and the ring will be buckling in the initial plane of the curved beam under the load, $p_2 = -\bar{p}_2$. The out-of-plane components of force, moment, and displacement are zero, i.e., $t_1 = 0$, $m_2 = 0$, $m_3 = 0$, $U_1 = 0$, and $\phi = 0$. The internal force and moment at the onset of buckling, $t_{2(0)}$, $t_{3(0)}$, and $m_{1(0)}$, satisfy Eq. (4.11) and have the relation with critical load, $\bar{p}_{2(0)}$, as
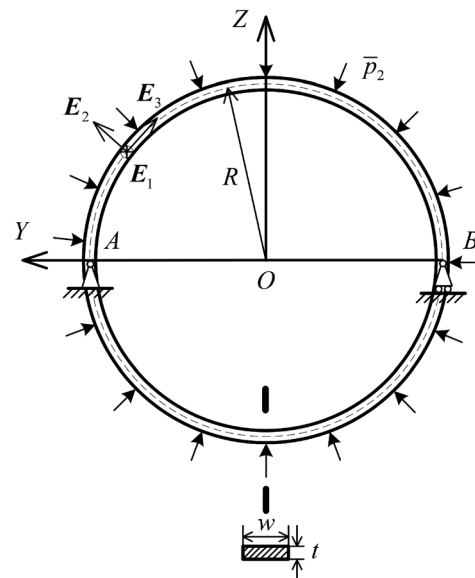

Fig. 2 Schematic illustration of elastic ring under uniform compression

$$t_{3(0)} = -\bar{p}_{2(0)}R, \quad t_{2(0)} = 0, \quad m_{1(0)} = 0 \qquad (5.4)$$

After substituting constitutive relation (4.10) into equilibrium equations (4.12) for $n = 1$ and eliminating $t_{2(1)}$ and $\hat{\kappa}_{1(1)}$, the differential equation for elongation, $\lambda_{(1)}$, is derived as

$$\frac{d^3 \lambda_{(1)}}{dS^3} + k_1^2 \frac{d\lambda_{(1)}}{dS} = 0 \qquad (5.5)$$

where $k_1^2 = [1 + \bar{p}_{2(0)}R/(EA) + \bar{p}_{2(0)}R^3/(EI_1)]/R^2$. Solution of Eq. (5.5) is

$$\lambda_{(1)} = C_{12} \cos(k_1 S) + C_{11} \sin(k_1 S) + C_{10} \qquad (5.6)$$

where C_{10}, C_{11}, and C_{12} are the parameters to be determined. The critical load, $\bar{p}_{2(0)}$, can be determined by the periodical condition of elongation, $\lambda_{(1)}$, as

$$\bar{p}_{2(0)} = \frac{3EI_1}{R^3}(1 + c_1)^{-1} \qquad (5.7)$$

where $c_1 = EI_1/(EAR^2)$. $\hat{\kappa}_{1(1)}$ is also obtained by substituting Eqs. (4.10) and (5.6) into Eq. (4.12) as

$$\hat{\kappa}_{1(1)} = \frac{1}{3Rc_1}\left\{ C_{10} + c_1 \left[\frac{\bar{p}_{2(1)}R^3}{EI_1}(1 + c_1) + 4C_{10} \right] \right. \\ \left. - 3\left(C_{11} \sin \frac{2S}{R} + C_{12} \cos \frac{2S}{R} \right) \right\} \qquad (5.8)$$

The differential equations for $U_{2(1)}$ and $U_{3(1)}$ can be derived from Eqs. (4.4) and (4.5) as

$$\frac{dU_{3(1)}}{dS} + \frac{U_{2(1)}}{R} = \lambda_{(1)} \\ \frac{d^2 U_{2(1)}}{dS^2} - \frac{1}{R}\frac{dU_{3(1)}}{dS} = -\hat{\kappa}_{1(1)} \qquad (5.9)$$

The solutions of $U_{2(1)}$ and $U_{3(1)}$ can be obtained by the boundary conditions (5.1) and (5.2) and the periodical condition (5.3) as
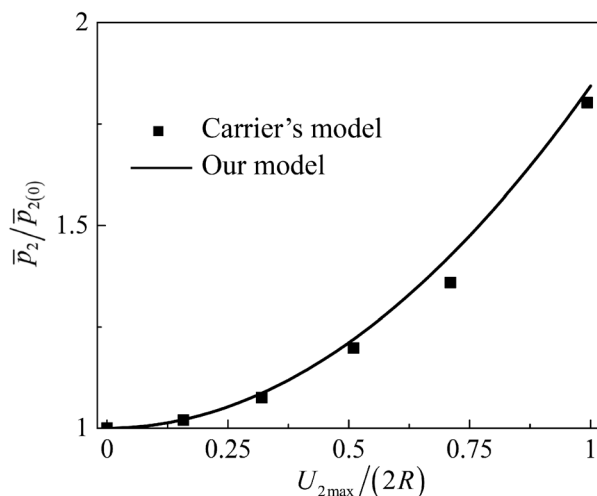

Fig. 3 The ratio of load to critical load, $\bar{p}_2/\bar{p}_{2(0)}$, versus the normalized displacement, $U_{2\text{max}}/(2R)$, during post-buckling, which is consistent with the results of Carrier's model

$$U_{2(1)} = -R\cos\frac{S}{R} + R\cos\frac{2S}{R} - \frac{(1 + c_1)c_1}{1 + 4c_1}\frac{\bar{p}_{2(1)}R^4}{EI_1}\left(1 - \cos\frac{2S}{R}\right)$$

$$U_{3(1)} = R\sin\frac{S}{R} - \frac{R}{2}\left(\frac{1 + 4c_1}{1 + c_1} + c_1\frac{\bar{p}_{2(1)}R^3}{EI_1}\right)\sin\frac{2S}{R}$$

$$(5.10)$$

and the parameters, C_{10}, C_{11}, and C_{12}, are also determined as

$$C_{10} = -\frac{\bar{p}_{2(1)}R^3}{EI_1}\frac{c_1(1 + c_1)}{1 + 4c_1}, \quad C_{11} = 0,$$

$$C_{12} = -\left[\frac{3c_1}{(1 + c_1)} + \frac{3c_1^2}{(1 + 4c_1)}\frac{\bar{p}_{2(1)}R^3}{EI_1}\right] \qquad (5.11)$$

where $U_{2(1)}$ is assumed to be symmetrical about AB, and $\max(U_{2(1)}) = 2R$.

Substitution of constitutive relation (4.10) into equilibrium equations (4.12) for $n = 2$ and elimination of $t_{2(2)}$ and $\hat{\kappa}_{1(2)}$ give the differential equation for elongation, $\lambda_{(2)}$, as

$$\frac{d^3 \lambda_{(2)}}{dS^3} + k_1^2 \frac{d\lambda_{(2)}}{dS} = F_{21}(S) \qquad (5.12)$$

where

$$F_{21}(S) = \frac{3\left[1 + 4c_1 + \frac{c_1\bar{p}_{2(1)}R^3}{EI_1}(1 + c_1)\right]}{R^3(1 + c_1)^2(1 + 4c_1)^2} \\ \left\{ \begin{array}{l} -\frac{2\bar{p}_{2(1)}R^3}{EI_1}c_1\left(1 + 3c_1^2 + 4c_1^3\right)\sin\frac{2S}{R} \\ -45c_1\left[1 + 4c_1 + \frac{\bar{p}_{2(1)}R^3}{EI_1}c_1(1 + c_1)\right]\sin\frac{4S}{R} \end{array} \right\}$$

The solution of Eq. (5.12) is

$$\lambda_{(2)} = C_{22}\cos(k_1 S) + C_{21}\sin(k_1 S) + C_{20} \\ + \int_0^S \int_0^\zeta \frac{\sin[k_1(S - \xi)]F_{21}(\xi)}{k_1} d\xi d\zeta \qquad (5.13)$$

where $\lambda_{(2)}$ is also periodical, which determined the increment of load, $\bar{p}_{2(1)} = 0$, and the parameters, C_{20}, C_{21}, and C_{22} will be determined with the boundary conditions and orthogonality condition [37,38], $\int_0^{2\pi R} \lambda_{(1)}(\xi)\lambda_{(2)}(\xi)d\xi = 0$.

The curvature, $\hat{\kappa}_{1(2)}$, is also obtained by substitution of Eqs. (4.10) and (5.13) into Eq. (4.12) as

$$\hat{\kappa}_{1(2)} = -\frac{3(23 + 68c_1)}{16R(1 + c_1)^2} + \frac{1 + c_1}{3R}\frac{\bar{p}_{2(2)}R^3}{EI_1} + \frac{1 + 4c_1}{3Rc_1}C_{20} - \frac{C_{21}}{Rc_1}\sin\frac{2S}{R} \\ - \frac{1}{4R}\left[\frac{45}{(1 + c_1)^2} + \frac{4C_{22}}{c_1}\right]\cos\frac{2S}{R} + \frac{9(1 - 4c_1)}{16R(1 + c_1)^2}\cos\frac{4S}{R}$$

$$(5.14)$$

The differential equations for $U_{2(2)}$ and $U_{3(2)}$ are given by substitution of Eqs. (5.13) and (5.14) into Eqs. (B1) and (B2) as

$$\frac{d^2 U_{2(2)}}{dS^2} - \frac{1}{R}\frac{dU_{3(2)}}{dS} = F_{22}(S) \\ \frac{dU_{3(2)}}{dS} + \frac{U_{2(2)}}{R} = F_{23}(S) \qquad (5.15)$$

where

$$F_{22}(S) = -\hat{\kappa}_{1(2)} + \underline{\left[\frac{\mathrm{d}}{\mathrm{d}S}\left(\frac{\mathrm{d}U_{3(1)}}{\mathrm{d}S}\frac{\mathrm{d}U_{2(1)}}{\mathrm{d}S} \right) + \frac{1}{2R}\frac{\mathrm{d}^2\left(U_{2(1)}^2 - U_{3(1)}^2\right)}{\mathrm{d}S^2} - \frac{1}{R^2}\frac{\mathrm{d}\left(U_{2(1)}U_{3(1)}\right)}{\mathrm{d}S} \right]}$$

$$F_{23}(S) = \lambda_{(2)} - \frac{1}{2}\left(\frac{\mathrm{d}U_{2(1)}}{\mathrm{d}S} - \frac{1}{R}U_{3(1)} \right)^2$$

and the underlined terms in $F_{22}(S)$ come from the nonlinear part of curvature (B2).

The solutions of Eq. (5.15) with the boundary conditions (5.1) and (5.2) are

$$U_{2(2)} = \frac{R}{80(1+c_1)^2(1+4c_1)}\left\{ \begin{array}{l} 180c_1(1+2c_1) - 3c_1(61+124c_1)\cos\dfrac{S}{R} \\ -5\left[9 + 16c_1(1+c_1)^3\dfrac{\bar{p}_{2(2)}R^3}{EI_1}\right]\left(1 - \cos\dfrac{S}{R}\right) + 3c_1(1+4c_1)\cos\dfrac{4S}{R} \end{array} \right\}$$
$$\underline{+\frac{3Rc_1}{5(1+c_1)^2}\left(\cos\frac{S}{R} - \cos\frac{4S}{R}\right)}$$

$$U_{3(2)} = -\frac{R}{320(1+c_1)^2(1+4c_1)}\left\{ \begin{array}{l} 4\left[45 - 3c_1(61+124c_1) + 80c_1(1+c_1)^3\dfrac{\bar{p}_{2(2)}R^3}{EI_1}\right]\sin\dfrac{S}{R} \\ +3(1+4c_1)(-15+76c_1)\sin\dfrac{4S}{R} \end{array} \right\} \underline{+ \frac{3Rc_1}{20(1+c_1)^2}\left(-4\sin\frac{S}{R} + \sin\frac{4S}{R}\right)}$$

(5.16)

where the underlined terms are derived from the nonlinear terms of the curvature, and $U_{2(2)}$ is assumed to be symmetrical about AB. The parameters, C_{20}, C_{21}, and C_{22}, are also determined as

$$C_{20} = \frac{-c_1(1+c_1)}{(1+4c_1)}\frac{\bar{p}_{2(2)}R^3}{EI_1} + \frac{9c_1(23+68c_1)}{16(1+c_1)^2(1+4c_1)},$$

$$C_{21} = 0, \quad C_{22} = \frac{-45c_1}{4(1+c_1)^2}$$

(5.17)

Substitution of constitutive relation (4.10) into equilibrium equation (4.12) for $n = 3$ and elimination of $t_{2(3)}$ and $\hat{\kappa}_{1(3)}$ give the differential equation for elongation, $\lambda_{(3)}$, as

$$\frac{\mathrm{d}^3\lambda_{(3)}}{\mathrm{d}S^3} + k_1^2\frac{\mathrm{d}\lambda_{(3)}}{\mathrm{d}S} = F_3(S)$$

(5.18)

where

$$F_3(S) = \frac{6c_1}{R^3(1+c_1)(1+4c_1)}$$
$$\left[\frac{27(3-24c_1-16c_1^2)}{32(1+c_1)^2} - (1-c_1+4c_1^2)\frac{\bar{p}_{2(2)}R^3}{EI_1}\right]\sin\frac{2S}{R}$$
$$+\frac{1053c_1(-3+4c_1)}{16R^3(1+c_1)^3}\sin\frac{6S}{R}$$

The solution of Eq. (5.18) is

$$\lambda_{(3)} = C_{32}\cos(k_1 S) + C_{31}\sin(k_1 S) + C_{30}$$
$$+ \int_0^S\int_0^\zeta \frac{\sin[k_1(\zeta-\xi)]F_3(\xi)}{k_1}\mathrm{d}\xi\mathrm{d}\zeta$$

(5.19)

where C_{30}, C_{31}, and C_{32} are the parameters, and the increment of load, $\bar{p}_{2(2)}$, can be determined by the periodical condition of elongation, $\lambda_{(3)}$

$$\bar{p}_{2(2)} = \frac{(3-24c_1-16c_1^2)}{(1+c_1)^2(1-c_1+4c_1^2)}\frac{27EI_1}{32R^3}$$

(5.20)

The thickness, t, of the cross section of beam is much smaller than the radius, R, which indicates $c_1 \ll 1$. The load, $\bar{p}_2$, normalized by critical load, $\bar{p}_{2(0)}$, can be simplified as

$$\frac{\bar{p}_2}{\bar{p}_{2(0)}} = 1 + a^2\frac{\bar{p}_{2(2)}}{\bar{p}_{2(0)}} \approx 1 + \frac{27a^2}{32} = 1 + \frac{27}{32}\left(\frac{U_{2\max}}{2R}\right)^2$$

(5.21)

where $a = U_{2\max}/(2R)$ has been used, and it is the same with the result of Budiansky [33].

Figure 3 shows that the normalized load, $\bar{p}_2/\bar{p}_{2(0)}$, increases with the normalized maximum displacement, $U_{2\max}/(2R)$, which is consistent with Carrier's model [32]. It indicates that the elongation can be neglected due to the inextensibility of elastic ring in Carrier's model.

6 Lateral Buckling of Circular Beam

The curved beam is widely used as interconnector, which is often freestanding and connects the sensors in the stretchable and

flexible electronics [2]. The lateral buckling of the freestanding interconnector will happen because the thickness of the beam cross section, t, is much larger than its width, w [1,2,16]. The thickness direction is along the radial direction of the circular beam, which is consistent with it in Sec. 5. The displacement, U_1, and rotation, ϕ, which are the odd powers of the small ratio, a, of the maximum deflect of U_1 to beam length, are the primary displacements, while the secondary displacements, U_2 and U_3, are the even powers of the small ratio, a [41]. The curvatures, $\hat{\kappa}_2$ and $\hat{\kappa}_3$, are the odd powers of the small ratio, a, and the elongation, λ, and curvature, $\hat{\kappa}_1$, are the even powers of the small ratio, a.

6.1 The Lateral Buckling of Circular Beam Under Bending Moment.
As shown in Fig. 4, the bending moment, M, is applied on the circular beam at the ends. This beam with length, L_S, which subtends the angle, α, is simply supported in the plane and the out-of-plane, and beam ends cannot rotate around the centroid of beam, but the right beam end can freely slide in the plane of the beam, i.e.,

$$U_2|_{S=0} = U_3|_{S=0} = 0$$
$$(U_2 \boldsymbol{E}_2 + U_3 \boldsymbol{E}_3)|_{S=L_S} \cdot \left(\cos \frac{\alpha}{2} \boldsymbol{E}_2 - \sin \frac{\alpha}{2} \boldsymbol{E}_3 \right)\bigg|_{S=L_S} = 0$$
$$\boldsymbol{t}|_{S=L_S} \cdot \left(\sin \frac{\alpha}{2} \boldsymbol{E}_2 + \cos \frac{\alpha}{2} \boldsymbol{E}_3 \right)\bigg|_{S=L_S} = 0 \quad (6.1)$$
$$m_1|_{S=0} = m_1|_{S=L_S} = M$$

$$U_1|_{S=0} = U_1|_{S=L_S} = 0$$
$$(\boldsymbol{e}_2 \cdot \boldsymbol{E}_1)|_{S=0} = (\boldsymbol{e}_2 \cdot \boldsymbol{E}_1)|_{S=L_S} = 0 \quad (6.2)$$
$$m_2|_{S=0} = m_2|_{S=L_S} = 0$$

By substituting Eq. (3.2) into the above equations, the boundary conditions can be expanded with respect to the perturbation parameter, a, as

$$U_{2(n)}|_{S=0} = U_{3(n)}|_{S=0} = 0$$
$$\left(U_{2(n)} \cos \frac{\alpha}{2} - U_{3(n)} \sin \frac{\alpha}{2} \right)\bigg|_{S=L_S} = 0$$
$$\sum_{l=0}^{l=n} \left(t_{i(l)} a_{i2(n-l)} \sin \frac{\alpha}{2} + t_{i(l)} a_{i3(n-l)} \cos \frac{\alpha}{2} \right)\bigg|_{S=L_S} = 0 \quad (6.3)$$
$$m_{1(n)}|_{S=0} = m_{1(n)}|_{S=L_S} = M_{(n)}$$

$$U_{1(n)}|_{S=0} = U_{1(n)}|_{S=L_S} = 0$$
$$a_{21(n)}|_{S=0} = a_{21(n)}|_{S=L_S} = 0 \quad (6.4)$$
$$m_{2(n)}|_{S=0} = m_{2(n)}|_{S=L_S} = 0$$

The internal forces and moments at the onset of buckling, $t_{i(0)}$, $m_{i(0)}(i=1,2,3)$, satisfy Eq. (4.11) and have the relation with critical load, $M_{(0)}$, as

$$t_{1(0)} = t_{2(0)} = t_{3(0)} = 0, \; m_{2(0)} = m_{3(0)} = 0, \; m_{1(0)} = M_{(0)} \quad (6.5)$$

Substitution of constitutive relation (4.10) into equilibrium equations (4.12) for $n=1$ and elimination of $\hat{\kappa}_{3(1)}$ and $t_{1(1)}$ give the differential equation for $\hat{\kappa}_{2(1)}$ as

$$\frac{d^2 \hat{\kappa}_{2(1)}}{dS^2} + k_2^2 \hat{\kappa}_{2(1)} = 0 \quad (6.6)$$

where $k_2^2 = [M_{(0)}R/(EI_2) - 1][(M_{(0)}Rc_2/(EI_2) - c_3)/(R^2 c_3)]$, $c_2 = EI_2/(EAR^2)$, and $c_3 = GJ/(EAR^2)$. The solution of Eq. (6.6) is

$$\hat{\kappa}_{2(1)} = C_{41} \cos (k_2 S) + C_{40} \sin (k_2 S) \quad (6.7)$$

where the parameters, C_{40} and C_{41}, will be determined by the boundary conditions. The boundary conditions, $\hat{\kappa}_{2(1)}|_{S=0} = \hat{\kappa}_{2(1)}|_{S=L_S} = 0$, which are derived by substitution of constitutive relation (4.10) into the boundary conditions (6.4), determine the critical load as

$$M_{(0)} = \frac{EI_2}{2R} \left[1 + \frac{c_3}{c_2} + \sqrt{\left(1 - \frac{c_3}{c_2}\right)^2 + \frac{4}{\bar{\alpha}^2} \frac{c_3}{c_2}} \right] \; \text{or}$$
$$M_{(0)} = \frac{EI_2}{2R} \left[1 + \frac{c_3}{c_2} - \sqrt{\left(1 - \frac{c_3}{c_2}\right)^2 + \frac{4}{\bar{\alpha}^2} \frac{c_3}{c_2}} \right] \quad (6.8)$$

where the normalized angle, $\bar{\alpha} = \alpha/\pi$, and k_2 can be simplified to $1/(R\bar{\alpha})$. When $\bar{\alpha} = 1$, one of the two values of the critical load in Eq. (6.8) is zero, which corresponds to the freedom of a semicircular beam to rotate about the diameter connecting the two ends, the other value, $M_{(0)} = \pi EI_2(1 + c_3/c_2)/L_S$, is the critical load for the semicircular beam. When the curved beam is shallow, i.e., $R \gg L_S$, the critical load, $M_{(0)}$, will approach to the critical load for the straight beam, $(\pi EI_2/L_S)\sqrt{c_3/c_2}$ [31].

The $\hat{\kappa}_{3(1)}$ can be obtained by the substitution of constitutive relation (4.10) and Eq. (6.7) into equilibrium equations (4.12) for $n=1$ as

$$\hat{\kappa}_{3(1)} = \frac{\bar{\alpha} c_2}{c_3} \left(\frac{M_{(0)}R}{EI_2} - 1 \right) \left[C_{40} \left(1 - \cos \frac{S}{\bar{\alpha}R} \right) + C_{41} \sin \frac{S}{\bar{\alpha}R} \right] + C_{42} \quad (6.9)$$

where the parameter, C_{42}, will be determined by the boundary condition.

The differential equations for $U_{1(1)}$ and $\phi_{(1)}$ can be derived from Eq. (4.5) as

$$\frac{d\phi_{(1)}}{dS} = \hat{\kappa}_{3(1)}$$
$$\frac{d^2 U_{1(1)}}{dS^2} + \frac{1}{R^2} U_{1(1)} = \hat{\kappa}_{2(1)} + \frac{1}{R} \phi_{(1)} \quad (6.10)$$

The solutions of Eq. (6.10), which satisfy the boundary conditions (6.4), are

$$\phi_{(1)} = \frac{\pi c_2 \bar{\alpha}(\bar{\alpha}^2 - 1)\left(\dfrac{M_{(0)}R}{EI_2} - 1\right)}{\bar{\alpha}^2 c_2 \left(\dfrac{M_{(0)}R}{EI_2} - 1\right) - c_3} \sin \frac{S}{\bar{\alpha}R}$$
$$U_{1(1)} = \pi \bar{\alpha} R \sin \frac{S}{\bar{\alpha}R} \quad (6.11)$$

where the maximum of $U_{1(1)}$ is L_S, and the parameters, C_{40}, C_{41}, and C_{42}, are

$$C_{40} = \frac{\pi}{\bar{\alpha}R} \frac{c_3(\bar{\alpha}^2 - 1)}{c_3 + \bar{\alpha}^2 c_2 \left(1 - \dfrac{M_{(0)}R}{EI_2}\right)}, \; C_{41} = 0,$$
$$C_{42} = \frac{\pi}{R} \frac{c_2(\bar{\alpha}^2 - 1)\left(1 - \dfrac{M_{(0)}R}{EI_2}\right)}{c_3 + \bar{\alpha}^2 c_2 \left(1 - \dfrac{M_{(0)}R}{EI_2}\right)} \quad (6.12)$$

Substitution of constitutive relation (4.10) into equilibrium equations (4.12) for $n=2$ and elimination of $\lambda_{(2)}$ and $t_{2(2)}$ give the differential equation for leading terms of $\hat{\kappa}_1$ and $\hat{\kappa}_{1(2)}$, as

$$\frac{\mathrm{d}^3 \hat{\kappa}_{1(2)}}{\mathrm{d}S^3} + k_3^2 \frac{\mathrm{d}\hat{\kappa}_{1(2)}}{\mathrm{d}S} = F_{51}(S) \tag{6.13}$$

where $k_3^2 = 1/R^2$, and $F_{51}(S) = (c_2 - c_3)/c_1[(\mathrm{d}^2/\mathrm{d}S^2)(\hat{\kappa}_{2(1)}\hat{\kappa}_{3(1)}) + (1/R^2)\hat{\kappa}_{2(1)}\hat{\kappa}_{3(1)}]$. The solution of Eq. (6.13) is

$$\hat{\kappa}_{1(2)}(S) = C_{52}\cos(k_3 S) + C_{51}\sin(k_3 S) + C_{50} + \int_0^S \int_0^\zeta \frac{\sin[k_3(\zeta - \xi)]F_{51}(\xi)}{k_3} \mathrm{d}\xi \mathrm{d}\zeta \tag{6.14}$$

The elongation, $\lambda_{(2)}$, can be obtained by substitution of constitutive relation (4.10) and the above equation into equilibrium equations (4.12) for $n = 2$ as

$$\lambda_{(2)} = -c_1 R\left(C_{52}\cos\frac{S}{R} + C_{51}\sin\frac{S}{R}\right) + \frac{\pi^2 c_2 c_3 (c_2 - c_3)(\bar{\alpha}^2 - 1)^2 \left(\dfrac{M_{(0)}R}{EI_2} - 1\right)}{\left[c_3\bar{\alpha} - c_2\bar{\alpha}^3 \left(\dfrac{M_{(0)}R}{EI_2} - 1\right)\right]^2}\cos\frac{2S}{\bar{\alpha}R}$$

$$+ c_1 R^3 \int_0^S \cos\frac{S - \xi}{R} F_{51}(\xi)\mathrm{d}\xi \tag{6.15}$$

The differential equations for the leading terms, $U_{2(2)}$ and $U_{3(2)}$, of displacements, U_2 and U_3, are derived by substitution of Eq. (6.14) into Eqs. (B1) and (B2) as

$$\frac{\mathrm{d}^2 U_{2(2)}}{\mathrm{d}S^2} + \frac{U_{2(2)}}{R^2} = F_{52}(S)$$

$$\frac{\mathrm{d}U_{3(2)}}{\mathrm{d}S} = \lambda_{(2)} - \frac{U_{2(2)}}{R} - \frac{1}{2}\left(\frac{\mathrm{d}U_{1(1)}}{\mathrm{d}S}\right)^2 \tag{6.16}$$

where

$$F_{52}(S) = -\hat{\kappa}_{1(2)} + \lambda_{(2)}/R - (\mathrm{d}U_{1(1)}/\mathrm{d}S)^2/(2R) + \underline{\psi_{(1)}^{[1]}(\mathrm{d}^2 U_{1(1)}/\mathrm{d}S^2) - \left[\left(\psi_{(1)}^{[1]}\right)^2 + (\mathrm{d}U_{1(1)}/\mathrm{d}S)^2\right]/(2R)}$$

and the underlined terms are derived from the nonlinear terms of curvature.

The solutions of Eq. (6.16), which satisfy the boundary conditions (6.3), are

$$U_{2(2)}(S) = C_{53}\cos\frac{S}{R} + C_{54}\sin\frac{S}{R} + R\int_0^S \sin\frac{(S - \xi)}{R} F_{52}(\xi)\mathrm{d}\xi,$$

$$U_{3(2)}(S) = \int_0^S \left[\lambda_{(2)}(\xi) - \frac{1}{R}U_{2(2)}(\xi) - \frac{1}{2}\left(\frac{\mathrm{d}U_{1(1)}(\xi)}{\mathrm{d}\xi}\right)^2\right]\mathrm{d}\xi + C_{55} \tag{6.17}$$

and the parameters, C_{50}, C_{51}, C_{52}, C_{53}, C_{54}, and C_{55}, are determined as

$$C_{55} = C_{53} = C_{51} = 0$$

$$C_{52} = \frac{\pi^2 \dfrac{c_2}{c_1}\left(\dfrac{c_2}{c_3} - 1\right)(\bar{\alpha}^2 - 1)^2 \left(\dfrac{M_{(0)}R}{EI_2} - 1\right)}{\bar{\alpha}^2 R\left[1 - \bar{\alpha}^2 \dfrac{c_2}{c_3}\left(\dfrac{M_{(0)}R}{EI_2} - 1\right)\right]^2}$$

$$C_{54} = -\frac{\pi\bar{\alpha}^3 R^2}{8}C_{52} + \frac{\pi\bar{\alpha}R}{2}\frac{c_2}{c_1}\frac{M_{(2)}R}{EI_2} + \frac{\pi^3(\bar{\alpha}^2 - 1)R}{8\bar{\alpha}}\left\{1 + \underline{\frac{\bar{\alpha}^2 - 1}{\left[1 - \bar{\alpha}^2 \dfrac{c_2}{c_3}\left(\dfrac{M_{(0)}R}{EI_2} - 1\right)\right]^2}}\right\} \tag{6.18}$$

$$C_{50} = -C_{52} + \frac{c_2}{Rc_1}\frac{M_{(2)}R}{EI_2}$$

Substitution of constitutive relation (4.10) into equilibrium equations (4.12) for $n = 3$ and elimination of $\hat{\kappa}_{3(3)}$ and $t_{1(3)}$ give the differential equation for $\hat{\kappa}_{2(3)}$ as

$$\frac{\mathrm{d}^2 \hat{\kappa}_{2(3)}}{\mathrm{d}S^2} + k_2^2 \hat{\kappa}_{2(3)} = F_6(S) \tag{6.19}$$

where

$$F_6(S) = \{(1 - c_1/c_2)[M_{(0)}Rc_2/(EI_2 c_3) - 1]\hat{\kappa}_{1(2)}\hat{\kappa}_{2(1)} - R(c_1/c_2 - c_3/c_2)[\mathrm{d}(\hat{\kappa}_{1(2)}\hat{\kappa}_{3(1)})/\mathrm{d}S]\}/R$$

The solution of Eq. (6.19) is

$$\hat{\kappa}_{2(3)} = C_{61}\cos(k_2 S) + C_{60}\sin(k_2 S) + \int_0^S \frac{\sin[k_2(S-\xi)]F_6(\xi)}{k_2}\,\mathrm{d}\xi \tag{6.20}$$

where C_{60} and C_{61} are the parameters. $\hat{\kappa}_{2(3)}$ satisfies the boundary conditions $\hat{\kappa}_{2(3)}|_{S=0} = \hat{\kappa}_{2(3)}|_{S=L_S} = 0$, which determine the load increment

$$M_{(2)} = \frac{EI_2}{R}\frac{\pi^2(\bar{\alpha}^2-1)^2\left(\frac{c_2}{c_3}-1\right)\left[1+3\frac{c_3}{c_2}-4\frac{c_3}{c_1}-\left(4-\frac{c_3}{c_1}-3\frac{c_2}{c_1}\right)\frac{M_{(0)}R}{EI_2}\right]\left(1-\frac{M_{(0)}R}{EI_2}\right)}{8\left[\left(1-\frac{M_{(0)}R}{EI_2}\right)\bar{\alpha}^2\frac{c_2}{c_3}+1\right]^2\left[2\frac{c_3}{c_1}-\frac{c_3}{c_2}-1+\left(2-\frac{c_2+c_3}{c_1}\right)\frac{M_{(0)}R}{EI_2}\right]} \tag{6.21}$$

For the narrow rectangular section of beam, which thickness is much larger than its width, i.e., $t \gg w$, the stiffness ratios, c_2 and c_3 are much smaller than c_1, i.e., $c_1 \gg c_2 \sim c_3$. The load increment in Eq. (6.21) can be simplified to

$$M_{(2)} \approx \frac{EI_2}{R}\frac{\pi^2(\bar{\alpha}^2-1)^2\left(\frac{c_2}{c_3}-1\right)\left(1+3\frac{c_3}{c_2}-4\frac{M_{(0)}R}{EI_2}\right)\left(1-\frac{M_{(0)}R}{EI_2}\right)}{8\left[\left(1-\frac{M_{(0)}R}{EI_2}\right)\bar{\alpha}^2\frac{c_2}{c_3}+1\right]^2\left(2\frac{M_{(0)}R}{EI_2}-1-\frac{c_3}{c_2}\right)} \tag{6.22}$$

The ratio of c_3 to c_2 is $2/(1+\nu)$, which only depends on the Poisson's ratio, Eq. (6.22) can be written as $M_{(2)} \approx (EI_2/R)f_1(\alpha,\nu)$. The ratio of bending moment load, M, to the critical load, $M_{(0)}$, is

$$\frac{M}{M_{(0)}} = 1 + a^2\frac{M_{(2)}}{M_{(0)}} \approx 1 + \left(\frac{U_{1\max}}{L_S}\right)^2\frac{\pi^2(\nu-1)(\bar{\alpha}^2-1)^2\left(\frac{7+\nu}{1+\nu}-\frac{4M_{(0)}R}{EI_2}\right)\left(1-\frac{M_{(0)}R}{EI_2}\right)}{4\frac{M_{(0)}R}{EI_2}\left[\bar{\alpha}^2(1+\nu)\left(1-\frac{M_{(0)}R}{EI_2}\right)+2\right]^2\left(\frac{2M_{(0)}R}{EI_2}-\frac{3+\nu}{1+\nu}\right)} \tag{6.23}$$

where the small ratio was defined as $a = U_{1\max}/L_S$.

The maximum principal strain in the beam can be obtained as

$$\varepsilon_{\max} = (aw)\max\left[\frac{1-\nu}{4}\left|\hat{\kappa}_{2(1)}\right| + \frac{1}{2}\left|\sqrt{\frac{(1-\nu)^2}{4}\hat{\kappa}_{2(1)}^2 + \hat{\kappa}_{3(1)}^2}\right|\right] \tag{6.24}$$

The shortening ratio of the distance, γ_d, between the beam ends due to the bending moment is defined as

$$\gamma_d = \frac{|U|_{S=L_S}|}{2R\sin\frac{\pi\bar{\alpha}}{2}} = \frac{a^2}{2R}\left|\left(U_{2(2)} + U_{3(2)}\cot\frac{\pi\bar{\alpha}}{2}\right)_{S=L_S}\right| \tag{6.25}$$

The ratio of the maximum principal strain in beam to $\sqrt{\gamma_d}(w/R)$ is

$$\gamma_\varepsilon = \frac{\varepsilon_{\max}}{\sqrt{\gamma_d}}\frac{R}{w} = f_2(\bar{\alpha},\nu) \tag{6.26}$$

where the function, $f_2(\bar{\alpha},\nu)$, depends only on the shape and the Poisson's ratio of beam. As shown in Fig. 5(a), the effect of Poisson's ratio on the ratio, γ_ε, can be neglected, especially for the curvature with the nonlinear terms. But the effect of the normalized angle, $\bar{\alpha}$, on the ratio, γ_ε, is significant as shown in Fig. 5(b), where the Poisson's ratio is 0.42 for gold, which is the primary material of the interconnector in the stretchable and flexible electronics. The value gap between the ratio, γ_ε, with and without the nonlinear terms in curvature would be larger than 100% for $\bar{\alpha} > 5/6$. Figure 6 shows the normalized maximum principal strain, $\varepsilon_{\max}R/w$, versus the shortening ratio of the ends distance, γ_d, for $\nu = 0.42$, which indicates that the nonlinear terms in curvatures should be considered for the strain of beam. There is 73% increase in the normalized maximum strain, $\varepsilon_{\max}R/w$, without the nonlinear terms of curvature for $\bar{\alpha} = 2/3$ and $\gamma_d = 0.3$ from the
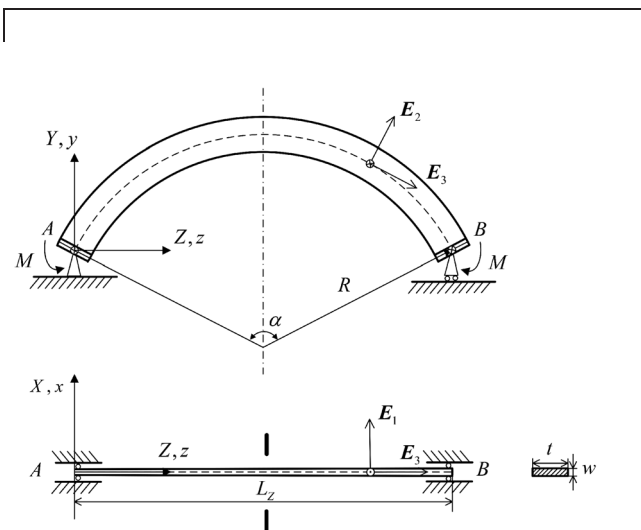

Fig. 4 Schematic illustration of boundary conditions of circular beam under bending moment load
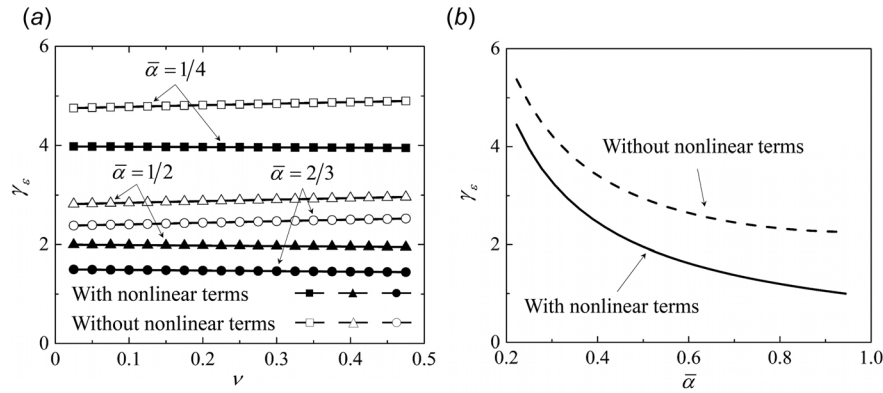
Fig. 5 The ratio, γ_ε, with and without the nonlinear terms in curvature: (a) the ratio, γ_ε, versus the Poisson's ratio ν for the normalized angle $\bar{\alpha} = 1/4$, $1/2$, and $2/3$. (b) The ratio, γ_ε, versus the normalized angle $\bar{\alpha}$ for gold (i.e., $\nu = 0.42$).

normalized maximum principal strain with the nonlinear terms, which indicates that the stretchability of circular beam is underestimated when the nonlinear terms are neglected. Figure 6 also shows that the relation between the normalized strain, $\varepsilon_{\max}R/w$, and the shortening ratio, γ_d, depends on the normalized angle, $\bar{\alpha}$, and the longer circular beams have the higher stretchability with the same critical normalized strain. This model can be used to analyze the stretchability of the serpentine bridge, which can be simplified as two semicircular beams [2]. The maximum strain in the bridge fabricated with gold can be obtained as $\varepsilon_{\max} = 0.9365$ $(w/R)\sqrt{\varepsilon_{\mathrm{pre}}/(1+\varepsilon_{\mathrm{pre}})}$ and $\varepsilon_{\max} = 2.264(w/R)\sqrt{\varepsilon_{\mathrm{pre}}/(1+\varepsilon_{\mathrm{pre}})}$ for the curvatures with and without the nonlinear terms, where the prestrain, $\varepsilon_{\mathrm{pre}}$, which is applied on the soft substrate, is related to the shortening ratio, γ_d, by $\varepsilon_{\mathrm{pre}} = \gamma_d/(1-\gamma_d)$. For the design of the stretchability of the serpentine bridge, the nonlinear terms of the curvature should be considered in the analysis process of the post-buckling behavior of the curved beam.

The finite-element method (FEM) of the commercial software ABAQUS, where the shell element S4R is used since the width of the cross section, w, is much smaller than its thickness, t, is adopted to simulate the post-buckling behaviors of the curved beams under the bending moments. The distributions of the twist angle ϕ of the circular beams for the shortening ratios, $\gamma_d = 0.1$, 0.2, and 0.3, are shown in Fig. 7, where the elastic modulus and Poisson's ratio are 79.5 GPa and 0.42 for gold, and the length, L_S, thickness, t, width, w, and the normal angle, $\bar{\alpha}$, of the circular

beam are 900 mm, 30 mm, 1 mm, and 2/3, respectively. Figure 7 shows that the theoretical results are consistent with the FEM results.

6.2 The Lateral Buckling of Circular Beams Under Uniform Pressure. As shown in Fig. 8, the uniform pressure, $\bar{p}_2 = -p_2$, which is along the thickness direction of cross section (i.e., $-e_2$) during the deformation, is applied on the circular beam, the lateral buckling will happen because the thickness of the beam section, t, is much larger than its width, w. The power orders of displacements are similar to those in Sec. 6.1. The beam with length, L_S, which subtends the angle, α, is simply supported in the plane and out-of-plane, and the beam ends cannot rotate around the centroid of beam, but can freely slide toward the arch center in the plane, i.e.,

$$U_3|_{S=0} = U_3|_{S=L_S} = 0$$
$$m_1|_{S=0} = m_1|_{S=L_S} = 0 \qquad (6.27)$$
$$(t \cdot E_2)|_{S=0} = (t \cdot E_2)|_{S=L_S} = 0$$

$$U_1|_{S=0} = U_1|_{S=L_S} = 0$$
$$(e_2 \cdot E_1)|_{S=0} = (e_2 \cdot E_1)|_{S=L_S} = 0 \qquad (6.28)$$
$$m_2|_{S=0} = m_2|_{S=L_S} = 0$$

The deformation of the model is symmetrical about the midline (i.e., the dotted–dashed line in Fig. 8) to avoid the rigid movement. By substituting Eq. (3.2) into the above boundary conditions, the expanded formulas with respect to the perturbation parameter, a, of the boundary conditions (6.27) and (6.28) are

$$U_{3(n)}|_{S=0} = U_{3(n)}|_{S=L_S} = 0$$
$$m_{1(n)}|_{S=0} = m_{1(n)}|_{S=L_S} = 0$$
$$\sum_{l=0}^{l=n}(t_{i(l)}a_{i2(n-l)})\Big|_{S=0} = \sum_{l=0}^{l=n}(t_{i(l)}a_{i2(n-l)})\Big|_{S=L_S} = 0 \qquad (6.29)$$

$$U_{1(n)}|_{S=0} = U_{1(n)}|_{S=L_S} = 0$$
$$a_{21(n)}|_{S=0} = a_{21(n)}|_{S=L_S} = 0 \qquad (6.30)$$
$$m_{2(n)}|_{S=0} = m_{2(n)}|_{S=L_S} = 0$$

The formulas and solving of the governing equations are similar to those in Sec. 6.1. Replacing k_2, k_3, $F_{51}(S)$, $F_{52}(S)$, and $F_6(S)$ in Sec. 6.1 with the following $\bar{k}_2$, $\bar{k}_3$, $\bar{F}_{51}(S)$, $\bar{F}_{52}(S)$, and $\bar{F}_6(S)$, which are
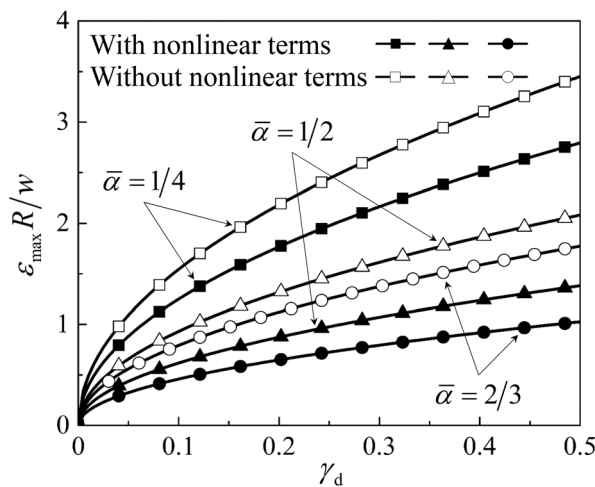

Fig. 6 The normalized maximum principal strain $\varepsilon_{\max}R/w$ with and without the nonlinear terms in curvature versus the shortening ratio γ_d for $\nu = 0.42$ and $\bar{\alpha} = 1/4$, $1/2$, and $2/3$

$$\bar{k}_2^2 = \frac{1}{R^2}\left(1 + \frac{\bar{p}_{2(0)}R^3}{EI_2}\right) \quad \bar{k}_3^2 = \frac{1}{R^2}\left[1 + \frac{c_2}{c_1}(1 + c_1)\frac{\bar{p}_{2(0)}R^3}{EI_2}\right] \tag{6.31}$$

$$\bar{F}_{51}(S) = \frac{1}{R^2 c_1}\left[\begin{array}{c} -2Rc_3\hat{\kappa}_{3(1)}\dfrac{d\hat{\kappa}_{3(1)}}{dS} + R^2(3c_2 - 2c_3)\dfrac{d\hat{\kappa}_{2(1)}}{dS}\dfrac{d\hat{\kappa}_{3(1)}}{dS} + R^2(2c_2 - c_3)\dfrac{d^2\hat{\kappa}_{2(1)}}{dS^2}\hat{\kappa}_{3(1)} \\[2mm] +c_2\hat{\kappa}_{2(1)}\left(1 + \dfrac{\bar{p}_{2(0)}R^3}{EI_2}c_2\right)\left(\hat{\kappa}_{3(1)} - R\dfrac{d\hat{\kappa}_{2(1)}}{dS}\right) + R^2(c_2 - c_3)\hat{\kappa}_{2(1)}\dfrac{d^2\hat{\kappa}_{3(1)}}{dS^2} \end{array}\right]$$

$$\bar{F}_{52}(S) = -\hat{\kappa}_{1(2)} + \frac{\lambda_{(2)}}{R} - \frac{1}{2R}\left(\frac{dU_{1(1)}}{dS}\right)^2 + \psi_{(1)}^{[1]}\frac{d^2U_{1(1)}}{dS^2} - \frac{1}{2R}\left[\left(\psi_{(1)}^{[1]}\right)^2 + \left(\frac{dU_{1(1)}}{dS}\right)^2\right] \tag{6.32}$$

$$\bar{F}_6(S) = \frac{1}{R^2 c_2}\left\{\begin{array}{c} \hat{\kappa}_{2(1)}\left[R^2(c_2 - c_3)\hat{\kappa}_{3(1)}^2 + \lambda_{(2)}\right] + R\hat{\kappa}_{1(2)}\left[(c_1 - c_2)\hat{\kappa}_{2(1)} + R(c_3 - c_1)\dfrac{d\hat{\kappa}_{3(1)}}{dS}\right] \\[2mm] -c_3 R\dfrac{d}{dS}\left(\lambda_{(2)}\hat{\kappa}_{3(1)}\right) + R^2 c_2\dfrac{d}{dS}\left(\lambda_{(2)}\dfrac{d\hat{\kappa}_{2(1)}}{dS}\right) + R^2(-2c_1 + c_3)\hat{\kappa}_{3(1)}\dfrac{d\hat{\kappa}_{1(2)}}{dS} \end{array}\right\}$$

The critical load, $\bar{p}_{2(0)} = EI_2/R^3(\bar{\alpha}^{-2} - 1)$, is obtained by the boundary conditions (6.30), which is consistent with the result of previous study [42]. When $1 \gg c_1 \gg c_2 \sim c_3$, the load increment can be simplified to

$$\bar{p}_{2(2)} = \frac{EI_2}{R^3}\left[f_{31}(\nu, \bar{\alpha}) + \underline{f_{32}(\nu, \bar{\alpha})}\right] \tag{6.33}$$

where

$$f_{31}(\nu, \bar{\alpha}) = \frac{\pi^2(1 - \bar{\alpha}^2)^2\left[\bar{\alpha}^4(17 - \nu)(1 + \nu) + 16(3 + 2\nu) - 2\bar{\alpha}^2(22 + 33\nu + \nu^2)\right]}{8\bar{\alpha}^2(\bar{\alpha}^2 - 4)\left[2 + \bar{\alpha}^2(1 + \nu)\right]^2}$$

$$f_{32}(\nu, \bar{\alpha}) = \frac{\pi^2(1 - \bar{\alpha}^2)^2\left[8 + 4\nu + \bar{\alpha}^2(1 + \nu)^2\right]\left[8(1 - \bar{\alpha}^2)(1 + \nu) + \pi\bar{\alpha}(\bar{\alpha}^2 - 4)(3 + \nu)\cot\frac{\pi\bar{\alpha}}{2}\right]}{16\bar{\alpha}^2(\bar{\alpha}^2 - 4)\left[2 + \bar{\alpha}^2(1 + \nu)\right]^2} \tag{6.34}$$

The function $f_{32}(\nu, \bar{\alpha})$ is derived from the nonlinear terms of curvature.

The ratio of the uniform pressure to the critical load is

$$\frac{\bar{p}_2}{\bar{p}_{2(0)}} = 1 + a^2\frac{\bar{p}_{2(2)}}{\bar{p}_{2(0)}} \approx 1 + \left(\frac{U_{1\text{max}}}{L_S}\right)^2\frac{\left[f_{31}(\nu, \bar{\alpha}) + \underline{f_{32}(\nu, \bar{\alpha})}\right]}{\bar{\alpha}^{-2} - 1} \tag{6.35}$$
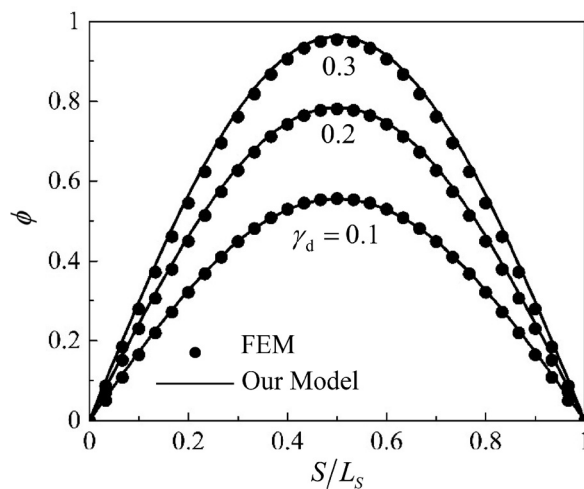

Fig. 7 The distributions of the twist angle of the circular beam for the different shortening ratios, γ_d = 0.1, 0.2, and 0.3
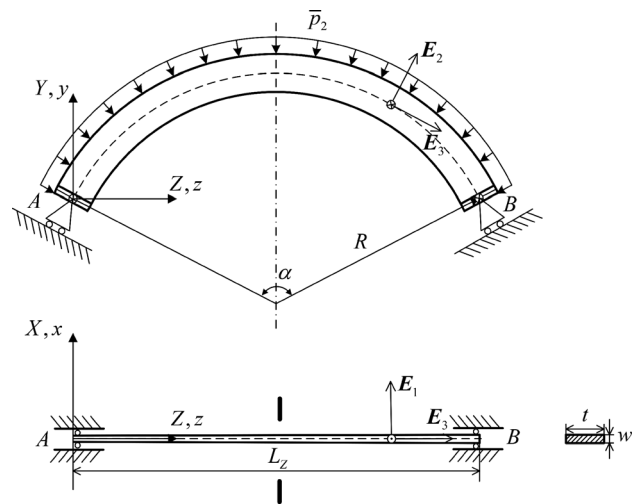

Fig. 8 Schematic illustration of boundary conditions of circular beam under uniform pressure
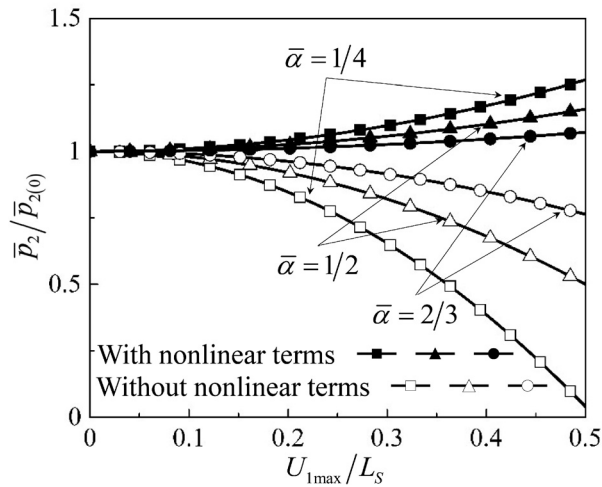
Fig. 9 The ratio of load to critical load, $\bar{p}_2/\bar{p}_{2(0)}$, with and without the nonlinear terms in curvature versus the normalized out-of-plane displacement, $U_{1\max}/L_S$, for $v = 0.42$ and $\bar{\alpha} = 1/4$, $1/2$, and $2/3$

Figure 9 shows the normalized load, $\bar{p}_2/\bar{p}_{2(0)}$, versus the normalized maximum displacement, $U_{1\max}/L_S$, which indicates that the nonlinear terms of curvature have significant impact on the analysis of the post-buckling behaviors of circular beam. The uniform pressure increases in the buckling process, but it decreases since the nonlinear terms of curvature is neglected.

7 Conclusions and Discussion

A systematic method is established for post-buckling analysis of curved beams in this paper. The deformation variables of the curved beam are up to the third power of generalized displacements due to the necessity of the fourth power of generalized displacements in the potential energy for the post-buckling analysis [37–39]. The currently prevailing post-buckling analyses, however, are accurate only to the second power of generalized displacements in the potential energy since some authors assume a linear displacement–curvature relation. Although the effect of the nonlinear terms of curvature on in-plane post-buckling behavior of planar beam is not so critical, it has significant impact on the

lateral post-buckling. When the bending moment is applied on circular beam, the strain in beam is overvalued ($\sim$73%) due to the neglect of the nonlinear terms in curvature expression, which will lead to underestimate of the stretchability of circular beam. The difference of post-buckling behavior also stems from the neglect of the nonlinear terms for the lateral buckling under the uniform pressure. In summary, the nonlinear terms in curvature can not be neglected in the lateral buckling behavior of the curved beam.

Acknowledgment

Appendix A

The second and third powers of generalized displacements in coefficients and curvatures are

$$
\begin{cases}
a_{11}^{\langle 2 \rangle} = -\dfrac{1}{2}\left[\left(\psi^{[1]}\right)^2 + U_1'^2\right] \\[2mm]
a_{12}^{\langle 2 \rangle} = -\dfrac{1}{2}U_1'U_2' + \dfrac{1}{2}U_1'U_3 K_1 + \psi^{[2]} \\[2mm]
a_{13}^{\langle 2 \rangle} = U_3'U_1' - \psi^{[1]}U_2' + \left(U_1'U_2 + \psi^{[1]}U_3\right)K_1
\end{cases}
\tag{A1}
$$

$$
\begin{cases}
a_{21}^{\langle 2 \rangle} = -\dfrac{1}{2}U_1'U_2' + \dfrac{1}{2}U_1'U_3 K_1 - \psi^{[2]} \\[2mm]
a_{22}^{\langle 2 \rangle} = -\dfrac{1}{2}\left[\left(\psi^{[1]}\right)^2 + \left(U_2' - U_3 K_1\right)^2\right] \\[2mm]
a_{23}^{\langle 2 \rangle} = \psi^{[1]}U_1' + \left(U_3' + U_2 K_1\right)\left(U_2' - U_3 K_1\right)
\end{cases}
\tag{A2}
$$

$$
\begin{cases}
a_{31}^{\langle 2 \rangle} = -\left(U_3' + U_2 K_1\right)U_1' \\[2mm]
a_{32}^{\langle 2 \rangle} = -\left(U_3' + U_2 K_1\right)\left(U_2' - U_3 K_1\right) \\[2mm]
a_{33}^{\langle 2 \rangle} = -\dfrac{1}{2}\left[U_1'^2 + \left(U_2' - U_3 K_1\right)^2\right]
\end{cases}
\tag{A3}
$$

$$
\begin{cases}
a_{11}^{\langle 3 \rangle} = -\dfrac{1}{2}\psi^{[1]}U_1'U_2' - \psi^{[1]}\psi^{[2]} + U_1'^2 U_3' + \left(U_1'^2 U_2 + \dfrac{1}{2}\psi^{[1]}U_1'U_3\right)K_1 \\[3mm]
a_{12}^{\langle 3 \rangle} = \dfrac{1}{4}\psi^{[1]}\left(U_1'^2 - U_2'^2\right) + U_1'U_2'U_3' + \psi^{[3]} \\[3mm]
\qquad + \left[U_1'\left(U_2'U_2 - U_3'U_3\right) + \dfrac{1}{2}\psi^{[1]}U_2'U_3\right]K_1 + \left(-\dfrac{1}{4}\psi^{[1]}U_3^2 - U_1'U_2 U_3\right)K_1^2 \\[3mm]
a_{13}^{\langle 3 \rangle} = \dfrac{1}{2}\left(\psi^{[1]}\right)^2 U_1' + \psi^{[1]}U_2'U_3' - \psi^{[2]}U_2' - U_1'\left[U_3'^2 - \dfrac{1}{2}\left(U_1'^2 + U_2'^2\right)\right] \\[3mm]
\qquad + \left[U_3\psi^{[2]} - \psi^{[1]}\left(U_3'U_3 - U_2'U_2\right) - U_1'\left(U_2'U_3 + 2U_2 U_3'\right)\right]K_1 \\[3mm]
\qquad + \left(-\psi^{[1]}U_2 U_3 + \dfrac{1}{2}U_1'U_3^2 - U_1'U_2^2\right)K_1^2
\end{cases}
\tag{A4}
$$

$$
\begin{cases}
a_{21}^{\langle 3\rangle} = \dfrac{1}{4}\psi^{[1]}\left(U_1'^2 - U_2'^2\right) + U_1'U_2'U_3' - \psi^{[3]} + \left[U_1'\left(U_2'U_2 - U_3'U_3\right) + \dfrac{1}{2}\psi^{[1]}U_2'U_3\right]K_1 + \left(-\dfrac{1}{4}\psi^{[1]}U_3^2 - U_1'U_2U_3\right)K_1^2 \\[2mm]
a_{22}^{\langle 3\rangle} = \dfrac{1}{2}\psi^{[1]}U_1'U_2' - \psi^{[1]}\psi^{[2]} + U_2'^2U_3' + \left(U_2U_2'^2 - \dfrac{1}{2}\psi^{[1]}U_1'U_3 - 2U_2'U_3'U_3\right)K_1 \\[2mm]
\qquad + \left(U_3'U_3^2 - 2U_2'U_2U_3\right)K_1^2 + U_2U_3^2K_1^3 \\[2mm]
a_{23}^{\langle 3\rangle} = \dfrac{1}{2}\left(\psi^{[1]}\right)^2 U_2' - \psi^{[1]}U_1'U_3' + \psi^{[2]}U_1' - U_2'\left[U_3'^2 - \dfrac{1}{2}\left(U_1'^2 + U_2'^2\right)\right] \\[2mm]
\qquad + \left\{-\psi^{[1]}U_1'U_2 - \dfrac{1}{2}U_3\left[\left(\psi^{[1]}\right)^2 + U_1'^2 + U_2'^2\right] + U_3\left(U_3'^2 - U_2'^2\right) - 2U_2U_2'U_3'\right\}K_1 \\[2mm]
\qquad + \left(2U_2U_3U_3' + \dfrac{3}{2}U_2'U_3^2 - U_2'U_2^2\right)K_1^2 + \left(U_2^2U_3 - \dfrac{1}{2}U_3^3\right)K_1^3
\end{cases} \tag{A5}
$$

$$
\begin{cases}
a_{31}^{\langle 3\rangle} = U_1'\left[U_3'^2 - \dfrac{1}{2}\left(U_1'^2 + U_2'^2\right)\right] + \left(U_1'U_2U_3 + 2U_1'U_2'U_3'\right)K_1 + \left(U_1'U_2 - \dfrac{1}{2}U_1'U_3^2\right)K_1^2 \\[2mm]
a_{32}^{\langle 3\rangle} = U_2'\left[U_3'^2 - \dfrac{1}{2}\left(U_1'^2 + U_2'^2\right)\right] + \left[\dfrac{1}{2}U_3\left(U_1'^2 + U_2'^2\right) + U_3\left(U_2'^2 - U_3'^2\right) + 2U_2U_2'U_3'\right]K_1 \\[2mm]
\qquad + \left(U_2'U_2^2 - 2U_2U_3U_3' - \dfrac{3}{2}U_2'U_3^2\right)K_1^2 + \left(\dfrac{1}{2}U_3^3 - U_2^2U_3\right)K_1^3 \\[2mm]
a_{33}^{\langle 3\rangle} = U_3'\left(U_1'^2 + U_2'^2\right) + \left[U_2\left(U_1'^2 + U_2'^2\right) - 2U_2'U_3'U_3\right]K_1 + \left(U_3'U_3^2 - 2U_2'U_2U_3\right)K_1^2 + U_2U_3^2K_1^3
\end{cases} \tag{A6}
$$

$$
\begin{cases}
\hat{\kappa}_1^{\langle 2\rangle} = \left\langle
\begin{array}{c}
\psi^{[1]}U_1'' + \left(U_3'U_2'\right)' + \left(U_2U_2' - U_3U_3'\right)K_1 \\[2mm]
+ \left\{\begin{array}{c}\left(U_2U_2'' - U_3U_3''\right) + \left(U_2'^2 - U_3'^2\right) \\[2mm] -\dfrac{1}{2}\left[\left(\psi^{[1]}\right)^2 + U_1'^2\right] - 2U_2U_3K_1'\end{array}\right\}K_1 - \left(U_2U_3\right)'K_1^2
\end{array}
\right\rangle \\[6mm]
\hat{\kappa}_2^{\langle 2\rangle} = \left[
\begin{array}{c}
\psi^{[1]}U_2'' - \left(U_3'U_1'\right)' - \left(\psi^{[1]}U_3 + U_1'U_2\right)K_1' \\[2mm]
-\left(\psi^{[1]}U_3' + \psi^{[2]} + U_1''U_2 + \dfrac{3}{2}U_1'U_2'\right)K_1 + \dfrac{1}{2}U_1'U_3K_1^2
\end{array}
\right] \\[6mm]
\hat{\kappa}_3^{\langle 2\rangle} = 0
\end{cases} \tag{A7}
$$

$$
\begin{cases}
\hat{\kappa}_1^{\langle 3\rangle} = \psi^{[2]}U_1'' + \dfrac{1}{2}\left(\psi^{[1]}\right)^2U_2'' - \psi^{[1]}\left(U_1''U_3' + U_1'U_3''\right) + U_2''\left(\dfrac{1}{2}U_1'^2 + U_2'^2 - U_3'^2\right) + \dfrac{1}{2}U_1''U_1'U_2' - 2U_3''U_2'U_3' \\[2mm]
\quad + \left\{U_3\left(U_3'^2 - U_2'^2\right) - \dfrac{1}{2}U_3\left[\left(\psi^{[1]}\right)^2 + U_1'^2\right] - U_2\left(\psi^{[1]}U_1' + 2U_2'U_3'\right)\right\}K_1' \\[2mm]
\quad + \left[\begin{array}{c} -\psi^{[1]}\psi^{[2]} - 2U_2\left(U_2'U_3'\right)' + \dfrac{1}{2}U_1'\left(U_1'U_3' - U_1''U_3\right) + \left(4U_2U_3U_3' + 2U_2'U_3^2 - 2U_2'U_2^2\right)K_1' \\[2mm] + U_3'^3 + 2U_3U_3'U_3'' - \dfrac{3}{2}U_1'U_2'\psi^{[1]} - U_1''U_2\psi^{[1]} - 2U_2'U_2''U_3 - 3U_2'^2U_3' - \dfrac{1}{2}U_3'\left(\psi^{[1]}\right)^2\end{array}\right]K_1 \\[2mm]
\quad + \left[\begin{array}{c} U_2''\left(U_3^2 - U_2^2\right) + 2U_2\left(U_3'^2 - U_2'^2\right) + \left(3U_2^2U_3 - U_3^3\right)K_1' \\[2mm] + 4U_2'U_3'U_3 + 2U_2U_3U_3'' + U_1'^2U_2 + \dfrac{1}{2}U_1'U_3\psi^{[1]}\end{array}\right]K_1^2 \\[2mm]
\quad + \left[U_3'\left(U_2^2 - U_3^2\right) + 2U_2U_2'U_3\right]K_1^3 \\[4mm]
\hat{\kappa}_2^{\langle 3\rangle} = \psi^{[2]}U_2'' - \dfrac{1}{2}\left(\psi^{[1]}\right)^2U_1'' - \psi^{[1]}\left(U_2''U_3' + U_2'U_3''\right) - U_1''\left(\dfrac{1}{2}U_2'^2 + U_1'^2 - U_3'^2\right) - \dfrac{1}{2}U_2''U_1'U_2' + 2U_3''U_1'U_3' \\[2mm]
\quad + \left[-\psi^{[1]}\left(U_2U_2' - U_3U_3'\right) - \psi^{[2]}U_3 + 2U_1'U_2U_3' + \dfrac{1}{2}U_1'U_2'U_3\right]K_1' \\[2mm]
\quad + \left[\begin{array}{c} \left(2U_1'U_2^2 - \dfrac{1}{2}U_1'U_3^2 + 2\psi^{[1]}U_2U_3\right)K_1' - \psi^{[1]}\left(\dfrac{5}{4}U_2'^2 - \dfrac{1}{4}U_1'^2 + U_2U_2'' - U_3U_3'' - U_3'^2\right) \\[2mm] -\psi^{[2]}U_3' - \psi^{[3]} + U_1''\left(U_2'U_3 + 2U_2U_3'\right) + U_1'\left(2U_2U_3'' + \dfrac{1}{2}U_2''U_3\right) + \dfrac{7}{2}U_1'U_2'U_3'\end{array}\right]K_1 \\[2mm]
\quad + \left[U_1''\left(U_2^2 - \dfrac{1}{2}U_3^2\right) - \dfrac{3}{2}U_3\left(U_1'U_3' - \psi^{[1]}U_2'\right) + \psi^{[1]}U_2U_3' + 3U_1'U_2U_2'\right]K_1^2 + \left(-\dfrac{1}{4}\psi^{[1]}U_3^2 - U_1'U_2U_3\right)K_1^3 \\[4mm]
\hat{\kappa}_3^{\langle 3\rangle} = 0
\end{cases} \tag{A8}
$$

where $()' = \mathrm{d}()/\mathrm{d}S$, and

$$\psi^{[2]} = \int \left[\frac{1}{2} \left(U'_1 U''_2 - U''_1 U'_2 \right) - U'_1 U_3 K'_1 + \frac{1}{2} \left(U'_1 U_3 K_1 \right)' + U'_1 U_2 K_1^2 \right] dS \tag{A9}$$

$$\psi^{[3]} = \int \left\{ \begin{array}{c} \left\{ -\frac{1}{2} \psi^{[1]'} \left(\psi^{[1]} \right)^2 + \frac{1}{4} \left[-\psi^{[1]} \left(U'^2_1 + U'^2_2 \right) \right]' + \left(U''_1 U'_2 - U'_1 U''_2 \right) U_3 \right\} \\[2mm] + \left(\frac{1}{2} \psi^{[1]} U'_2 U_3 + U'_1 U_3 U'_3 \right) K'_1 \\[3mm] + \left[\begin{array}{c} \frac{1}{2} \left(\psi^{[1]} U'_2 U_3 \right)' + \frac{1}{2} U'_1 \left(U'^2_1 + U'^2_2 \right) - U''_1 \left(U_3 U'_3 - U_2 U'_2 \right) - U'_1 U_2 U''_2 \\[2mm] + U_3 \left(U'_1 U_2 - \frac{1}{2} \psi^{[1]} U_3 \right) K'_1 \end{array} \right] K_1 \\[3mm] - \left[\left(U'_1 U_2 U_3 \right)' + U_3 \left(\frac{1}{2} \psi^{[1]} U'_3 + \frac{1}{4} \psi^{[1]'} U_3 \right) \right] K_1^2 - U'_1 \left(U_2^2 - \frac{1}{2} U_3^2 \right) K_1^3 \end{array} \right\} dS \tag{A10}$$

Appendix B

The expressions of $\lambda_{(2)}$, $\hat{\kappa}_{i(2)}$, and $a_{ij(2)}$ are

$$\lambda_{(2)} = U'_{3(2)} + U_{2(2)} K_1 + \frac{1}{2} \left[U'^2_{1(1)} + \left(U'_{2(1)} - U_{3(1)} K_1 \right)^2 \right] \tag{B1}$$

$$\left\{ \begin{array}{c} \hat{\kappa}_{1(2)} = \left\{ \begin{array}{c} -U''_{2(2)} + \left(U_{3(2)} K_1 \right)' + \psi^{[1]}_{(1)} U''_{1(1)} + \left(U'_{3(1)} U'_{2(1)} \right)' + \left(U_{2(1)} U'_{2(1)} - U_{3(1)} U'_{3(1)} \right) K'_1 \\[2mm] + \left\{ \begin{array}{c} \left(U_{2(1)} U''_{2(1)} - U_{3(1)} U''_{3(1)} \right) + \left(U'^2_{2(1)} - U'^2_{3(1)} \right) \\[2mm] - \frac{1}{2} \left[\left(\psi^{[1]}_{(1)} \right)^2 + U'^2_{1(1)} \right] - 2 U_{2(1)} U_{3(1)} K'_1 \end{array} \right\} K_1 - \left(U_{2(1)} U_{3(1)} \right)' K_1^2 \end{array} \right\} \\[8mm] \hat{\kappa}_{2(2)} = \left[\begin{array}{c} U''_{1(2)} - \psi^{[1]}_{(2)} K_1 + \psi^{[1]}_{(1)} U''_{2(1)} - \left(U'_{3(1)} U'_{1(1)} \right)' + \left(-\psi^{[1]}_{(1)} U_{3(1)} - U'_{1(1)} U_{2(1)} \right) K'_1 \\[2mm] + \left(-\psi^{[1]}_{(1)} U'_{3(1)} - \psi^{[2]}_{(2)} - U''_{1(1)} U_{2(1)} - \frac{3}{2} U'_{1(1)} U'_{2(1)} \right) K_1 + \frac{1}{2} U'_{1(1)} U_{3(1)} K_1^2 \end{array} \right] \\[6mm] \hat{\kappa}_{3(2)} = \phi'_{(2)} \end{array} \right. \tag{B2}$$

$$\left\{ \begin{array}{l} a_{11(2)} = -\frac{1}{2} \left[\left(\psi^{[1]}_{(1)} \right)^2 + U'^2_{1(1)} \right] \\[3mm] a_{12(2)} = \psi^{[1]}_{(2)} - \frac{1}{2} U'_{1(1)} U'_{2(1)} + \frac{1}{2} U'_{1(1)} U_{3(1)} K_1 + \psi^{[2]}_{(2)} \\[3mm] a_{13(2)} = -U'_{1(2)} + U'_{3(1)} U'_{1(1)} - \psi^{[1]}_{(1)} U'_{2(1)} + \left(U'_{1(1)} U_{2(1)} + \psi^{[1]}_{(1)} U_{3(1)} \right) K_1 \end{array} \right. \tag{B3}$$

$$\left\{ \begin{array}{l} a_{21(2)} = -\psi^{[1]}_{(2)} - \frac{1}{2} U'_{1(1)} U'_{2(1)} + \frac{1}{2} U'_{1(1)} U_{3(1)} K_1 - \psi^{[2]}_{(2)} \\[3mm] a_{22(2)} = -\frac{1}{2} \left[\left(\psi^{[1]}_{(1)} \right)^2 + \left(U'_{2(1)} - U_{3(1)} K_1 \right)^2 \right] \\[3mm] a_{23(2)} = -U'_{2(2)} + U_{3(2)} K_1 + \psi^{[1]}_{(1)} U'_{1(1)} + \left(U'_{3(1)} + U_{2(1)} K_1 \right) \left(U'_{2(1)} - U_{3(1)} K_1 \right) \end{array} \right. \tag{B4}$$

$$\left\{ \begin{array}{l} a_{31(2)} = U'_{1(2)} - \left(U'_{3(1)} + U_{2(1)} K_1 \right) U'_{1(1)} \\[3mm] a_{32(2)} = U'_{2(2)} - U_{3(2)} K_1 - \left(U'_{3(1)} + U_{2(1)} K_1 \right) \left(U'_{2(1)} - U_{3(1)} K_1 \right) \\[3mm] a_{33(2)} = -\frac{1}{2} \left[U'^2_{1(1)} + \left(U'_{2(1)} - U_{3(1)} K_1 \right)^2 \right] \end{array} \right. \tag{B5}$$

where $\psi^{[1]}_{(2)} = \phi_{(2)} - \int K_1 U'_{1(2)} dS$

$\psi^{[2]}_{(2)} = \int \left[\frac{1}{2} \left(U'_{1(1)} U''_{2(1)} - U''_{1(1)} U'_{2(1)} \right) - U'_{1(1)} U_{3(1)} K'_1 + \frac{1}{2} \left(U'_{1(1)} U_{3(1)} K_1 \right)' + U'_{1(1)} U_{2(1)} K_1^2 \right] dS.$

References

[1] Kim, D. H., Lu, N. S., Huang, Y. G., and Rogers, J. A., 2012, "Materials for Stretchable Electronics in Bioinspired and Biointegrated Devices," MRS Bull., **37**(3), pp. 226–235.

[2] Kim, D. H., Song, J. Z., Choi, W. M., Kim, H. S., Kim, R. H., Liu, Z. J., Huang, Y. Y., Hwang, K.-C., Zhang, Y. W., and Rogers, J. A., 2008, "Materials and Noncoplanar Mesh Designs for Integrated Circuits With Linear Elastic Responses to Extreme Mechanical Deformations," Proc. Natl. Acad. Sci. U.S.A., **105**(48), pp. 18675–18680.

[3] Lacour, S. P., Wagner, S., Narayan, R. J., Li, T., and Suo, Z. G., 2006, "Stiff Subcircuit Islands of Diamondlike Carbon for Stretchable Electronics," J. Appl. Phys., **100**(1), p. 014913.

[4] Lee, J., Wu, J., Ryu, J. H., Liu, Z., Meitl, M., Zhang, Y. W., Huang, Y., and Rogers, J. A., 2012, "Stretchable Semiconductor Technologies With High Areal Coverages and Strain-Limiting Behavior: Demonstration in High-Efficiency Dual-Junction Gainp/Gaas Photovoltaics," Small, **8**(12), pp. 1851–1856.

[5] Li, Y., Shi, X., Song, J., Lü, C., Kim, T.-I., Mccall, J. G., Bruchas, M. R., Rogers, J. A., and Huang, Y., 2013, "Thermal Analysis of Injectable, Cellular-Scale Optoelectronics With Pulsed Power," Proc. R. Soc. London A, **469**(2156), p. 20130398.

[6] Lin, S., Yuk, H., Zhang, T., Parada, G. A., Koo, H., Yu, C., and Zhao, X., 2016, "Stretchable Hydrogel Electronics and Devices," Adv. Mater., **28**(22), pp. 4497–4505.

[7] Lu, N. S., and Yang, S. X., 2015, "Mechanics for Stretchable Sensors," Curr. Opin. Solid State Mater. Sci., **19**(3), pp. 149–159.

[8] Ma, Q., and Zhang, Y., 2016, "Mechanics of Fractal-Inspired Horseshoe Microstructures for Applications in Stretchable Electronics," ASME J. Appl. Mech., **83**(11), p. 111008.

[9] Sekitani, T., Noguchi, Y., Hata, K., Fukushima, T., Aida, T., and Someya, T., 2008, "A Rubberlike Stretchable Active Matrix Using Elastic Conductors," Science, **321**(5895), pp. 1468–1472.

[10] Xu, S., Zhang, Y., Jia, L., Mathewson, K. E., Jang, K.-I., Kim, J., Fu, H., Huang, X., Chava, P., and Wang, R., 2014, "Soft Microfluidic Assemblies of Sensors, Circuits and Radios for the Skin," Science, **344**(6179), pp. 70–74.

[11] Xu, S., Zhang, Y. H., Cho, J., Lee, J., Huang, X., Jia, L., Fan, J. A., Su, Y. W., Su, J., Zhang, H. G., Cheng, H. Y., Lu, B. W., Yu, C. J., Chuang, C., Kim, T.-I., Song, T., Shigeta, K., Kang, S., Dagdeviren, C., Petrov, I., Braun, P. V., Huang, Y. G., Paik, U., and Rogers, J. A., 2013, "Stretchable Batteries With Self-Similar Serpentine Interconnects and Integrated Wireless Recharging Systems," Nat. Commun., **4**, p. 1543.

[12] Yang, S., Qiao, S., and Lu, N., 2016, "Elasticity Solutions to Nonbuckling Serpentine Ribbons," ASME J. Appl. Mech., **84**(2), p. 021004.

[13] Fan, Z., Zhang, Y., Ma, Q., Zhang, F., Fu, H., Hwang, K.-C., and Huang, Y., 2016, "A Finite Deformation Model of Planar Serpentine Interconnects for Stretchable Electronics," Int. J. Solids Struct., **91**, pp. 46–54.

[14] Cheng, H. Y., and Wang, S. D., 2014, "Mechanics of Interfacial Delamination in Epidermal Electronics Systems," ASME J. Appl. Mech., **81**(4), p. 044501.

[15] Jung, S., Kim, J. H., Kim, J., Choi, S., Lee, J., Park, I., Hyeon, T., and Kim, D. H., 2014, "Reverse-Micelle-Induced Porous Pressure-Sensitive Rubber for Wearable Human-Machine Interfaces," Adv. Mater., **26**(28), pp. 4825–4830.

[16] Kim, D. H., Lu, N. S., Ma, R., Kim, Y. S., Kim, R. H., Wang, S. D., Wu, J., Won, S. M., Tao, H., Islam, A., Yu, K. J., Kim, T. I., Chowdhury, R., Ying, M., Xu, L. Z., Li, M., Chung, H. J., Keum, H., Mccormick, M., Liu, P., Zhang, Y. W., Omenetto, F. G., Huang, Y. G., Coleman, T., and Rogers, J. A., 2011, "Epidermal Electronics," Science, **333**(6044), pp. 838–843.

[17] Lanzara, G., Salowitz, N., Guo, Z. Q., and Chang, F.-K., 2010, "A Spider-Web-Like Highly Expandable Sensor Network for Multifunctional Materials," Adv. Mater., **22**(41), pp. 4643–4648.

[18] Wang, S., Li, M., Wu, J., Kim, D. H., Lu, N., Su, Y., Kang, Z., Huang, Y., and Rogers, J. A., 2012, "Mechanics of Epidermal Electronics," ASME J. Appl. Mech., **79**(3), p. 031022.

[19] Kim, J., Lee, M., Shim, H. J., Ghaffari, R., Cho, H. R., Son, D., Jung, Y. H., Soh, M., Choi, C., Jung, S., Chu, K., Jeon, D., Lee, S. T., Kim, J. H., Choi, S. H., Hyeon, T., and Kim, D. H., 2014, "Stretchable Silicon Nanoribbon Electronics for Skin Prosthesis," Nat. Commun., **5**, p. 5747.

[20] Mannsfeld, S. C. B., Tee, B. C. K., Stoltenberg, R. M., Chen, C. V. H. H., Barman, S., Muir, B. V. O., Sokolov, A. N., Reese, C., and Bao, Z., 2010, "Highly Sensitive Flexible Pressure Sensors With Microstructured Rubber Dielectric Layers," Nat. Mater., **9**(10), pp. 859–864.

[21] Someya, T., Sekitani, T., Iba, S., Kato, Y., Kawaguchi, H., and Sakurai, T., 2004, "A Large-Area, Flexible Pressure Sensor Matrix With Organic Field-Effect Transistors for Artificial Skin Applications," Proc. Natl. Acad. Sci. U.S.A., **101**(27), pp. 9966–9970.

[22] Wagner, S., Lacour, S. P., Jones, J., Hsu, P. H. I., Sturm, J. C., Li, T., and Suo, Z. G., 2004, "Electronic Skin: Architecture and Components," Phys. E Low-Dimens. Syst. Nanostruct., **25**(2–3), pp. 326–334.

[23] Yang, S. X., Chen, Y. C., Nicolini, L., Pasupathy, P., Sacks, J., Su, B., Yang, R., Sanchez, D., Chang, Y. F., Wang, P. L., Schnyer, D., Neikirk, D., and Lu, N. S., 2015, "Cut-and-Paste" Manufacture of Multiparametric Epidermal Sensor Systems," Adv. Mater., **27**(41), pp. 6423–6430.

[24] Ko, H. C., Stoykovich, M. P., Song, J. Z., Malyarchuk, V., Choi, W. M., Yu, C.-J., Geddes, J. B., III, Xiao, J., Wang, S. D., Huang, Y. G., and Rogers, J. A., 2008, "A Hemispherical Electronic Eye Camera Based on Compressible Silicon Optoelectronics," Nature, **454**(7205), pp. 748–753.

[25] Lu, C. F., Li, M., Xiao, J. L., Jung, I., Wu, J., Huang, Y. G., Hwang, K.-C., and Rogers, J. A., 2013, "Mechanics of Tunable Hemispherical Electronic Eye Camera Systems That Combine Rigid Device Elements With Soft Elastomers," ASME J. Appl. Mech., **80**(6), p. 061022.

[26] Song, Y. M., Xie, Y. Z., Malyarchuk, V., Xiao, J. L., Jung, I., Choi, K.-J., Liu, Z. J., Park, H., Lu, C. F., Kim, R.-H., Li, R., Crozier, K. B., Huang, Y. G., and Rogers, J. A., 2013, "Digital Cameras With Designs Inspired by the Arthropod Eye," Nature, **497**(7447), pp. 95–99.

[27] Chen, C., Tao, W., Su, Y., Wu, J., and Song, J., 2013, "Lateral Buckling of Interconnects in a Noncoplanar Mesh Design for Stretchable Electronics," ASME J. Appl. Mech., **80**(4), p. 041031.

[28] Reis, P. M., 2015, "A Perspective on the Revival of Structural (in) Stability With Novel Opportunities for Function: From Buckliphobia to Buckliphilia," ASME J. Appl. Mech., **82**(11), p. 111001.

[29] Xu, S., Yan, Z., Jang, K. I., Huang, W., Fu, H., Kim, J., Wei, Z., Flavin, M., Mccracken, J., Wang, R., Badea, A., Liu, Y., Xiao, D., Zhou, G., Lee, J., Chung, H. U., Cheng, H., Ren, W., Banks, A., Li, X., Paik, U., Nuzzo, R. G., Huang, Y., Zhang, Y., and Rogers, J. A., 2015, "Assembly of Micro/Nanomaterials Into Complex, Three-Dimensional Architectures by Compressive Buckling," Science, **347**(6218), pp. 154–159.

[30] Yan, Z., Zhang, F., Liu, F., Han, M., Ou, D., Liu, Y., Lin, Q., Guo, X., Fu, H., Xie, Z., Gao, M., Huang, Y., Kim, J., Qiu, Y., Nan, K., Kim, J., Gutruf, P., Luo, H., Zhao, A., Hwang, K.-C., Huang, Y., Zhang, Y., and Rogers, J. A., 2016, "Mechanical Assembly of Complex, 3d Mesostructures From Releasable Multilayers of Advanced Materials," Sci. Adv., **2**(9), p. e1601014.

[31] Timoshenko, S. P., and Gere, J. M., 1961, *Theory of Elastic Stability*, 2nd ed., McGraw-Hill, New York.

[32] Carrier, G. F., 1947, "On the Buckling of Elastic Rings," J. Math. Phys., **26**(2), pp. 94–103.

[33] Budiansky, B., 1974, "Theory of Buckling and Post-Buckling Behavior of Elastic Structures," Adv. Appl. Mech., **14**, pp. 1–65.

[34] Liu, L., and Lu, N., 2016, "Variational Formulations, Instabilities and Critical Loadings of Space Curved Beams," Int. J. Solids Struct., **87**, pp. 48–60.

[35] Trahair, N. S., 1993, *Flexural-Torsional Buckling of Structures*, CRC Press, Boca Raton, FL.

[36] Trahair, N. S., and Papangelis, J. P., 1987, "Flexural-Torsional Buckling of Monosymmetric Arches," J. Struct. Eng., **113**(10), pp. 2271–2288.

[37] van der Heijden, A. M. A., 2009, *W.T. Koiter's Elastic Stability of Solids and Structures*, Cambridge University Press, New York.

[38] Koiter, W. T., 1963, "Elastic Stability and Post-Buckling Behaviour," *Nonlinear Problems*, University of Wisconsin Press, Madison, WI.

[39] Zhang, C., Wu, J., Hwang, K.-C., and Huang, Y., 2016, "Postbuckling of Hyperelastic Plates," ASME J. Appl. Mech., **83**(5), p. 051012.

[40] Love, A. E. H., 1927, *A Treatise on the Mathematical Theory of Elasticity*, Dover, New York.

[41] Su, Y., Wu, J., Fan, Z., Hwang, K.-C., Song, J., Huang, Y., and Rogers, J. A., 2012, "Postbuckling Analysis and Its Application to Stretchable Electronics," J. Mech. Phys. Solids, **60**(3), pp. 487–508.

[42] Challamel, N., Casandjian, C., and Lerbet, J., 2009, "On the Occurrence of Flutter in the Lateral–Torsional Instabilities of Circular Arches Under Follower Loads," J. Sound Vib., **320**(3), pp. 617–631.